



GEOHERMAL FIELD STUDIES USING STABLE ISOTOPE HYDROLOGY: CASE STUDIES IN UGANDA AND ICELAND

Vincent Kato

Geological Survey and Mines Department,
P. O. Box 9, Entebbe,
UGANDA
kato_vicent@hotmail.com

ABSTRACT

The first part of this report is a review of isotopic studies that have been carried out in the geothermal areas of Uganda for reservoir evaluation. Some new isotopic data from the Kibiro areas are also included. The second part of the report is a review of isotopic monitoring in the Svartsengi geothermal field, Iceland. Both case studies demonstrate the potential of isotopes to evaluate groundwater systems in combination with conventional geochemical methods. Isotopic analysis indicates that Uganda's geothermal water at Kibiro and Buranga is meteoric water that probably circulates to depth through fault systems, being heated and rising again. The origin of hot spring water at Buranga is at a higher altitude than the cold water and the whole area seems to have a single hot water reservoir. Relatively shallow and fast infiltration along permeable faults and fissures is inferred in this area. Very good agreement is observed for the two data sets (from 1994 and 2000) available for the isotopic composition of the water within the Kibiro area. It is suggested that the thermal water at Kibiro and the cold groundwater have a common origin, possibly local precipitation. An oxygen shift of about 1‰ is observed for the thermal water. Isotopic composition of Lake Albert is different from that of the hot springs, ruling out the possibility of direct recharge from the lake despite its close proximity. The geothermal water in Katwe is thought to be local and mixing is suggested between dilute cold groundwater and saline lake or dilute lake water.

According to chemical analyses the thermal water at Svartsengi, Iceland is 2/3 seawater and 1/3 local meteoric water. The isotopic composition of the thermal water deviates from such mixing in that it is enriched by about 0.5‰ in $\delta^{18}\text{O}$ and depleted by about 5‰ in δD . It is suggested that the deviation is due to water-rock interactions and possibly reflect previous stage when the hydrothermal fluid was more dilute. The $\delta^{18}\text{O}$ values exhibited a progressive increase in a southwesterly direction during the years 1984 and 1993. However, this trend changed between 1993-1994 to northeast. Well SG-6 was strongly influenced by nearby injection well SG-12. Temporal variation of $\delta^{18}\text{O}$ content in the geothermal fluids of individual wells indicates slight depletions in 1984 and 1994 attributed to boiling events.

1. INTRODUCTION

The present study was aimed to train the author in the application of isotope hydrology in geothermal resource development under the project 'Isotope hydrology for exploring geothermal resources (UGA/08/003) funded by the International Atomic Energy Agency (IAEA) and the government of Uganda. The first half of the report is a review of earlier isotopic work carried out in Uganda by Ármannsson (1994). It has been supplemented by new isotopic data from the Geological Survey and Mines Department, Isotope hydrology project. In this present investigation, the isotope hydrology technique is applied as an exploratory tool to hydrologically characterise the geothermal areas in Uganda for the purpose of assessing their potential. The second half is a review of isotopic monitoring studies in the Svartsengi geothermal field, SW-Iceland. The variation in the isotopic composition of geothermal fluids over time, as a result of production of reservoir fluids and injection of fresh water, is reviewed. The chemical composition in some producing wells has displayed the effects of dilution by injected fluids.

2. A REVIEW OF GEOTHERMAL RESERVOIR EVALUATION USING STABLE ISOTOPE HYDROLOGY: CASE STUDY IN UGANDA

2.1 Introduction

Exploration of natural hot water in western Uganda dates back to 1930, when the Geological Survey made brief reconnaissance investigations of the geothermal resources. Three prospects, namely, Katwe, Kibiro and Buranga located in the western rift valley (Figure 1), were identified by studies carried out from 1950's into the 1970's.

The United Nations/DTCD adviser, Stefánsson (1989), reviewed earlier studies and proposed a reconnaissance survey. The geothermal reconnaissance project started in March 1993 and lasted for 1.5 years. UNDP, OPEC and the governments of Iceland and Uganda funded the project. This phase of the project, which involved geological and geochemical methods, was to identify specific areas and assign them priorities for more detailed investigation. The second phase of the project will use data from the first phase and create a geothermal model.

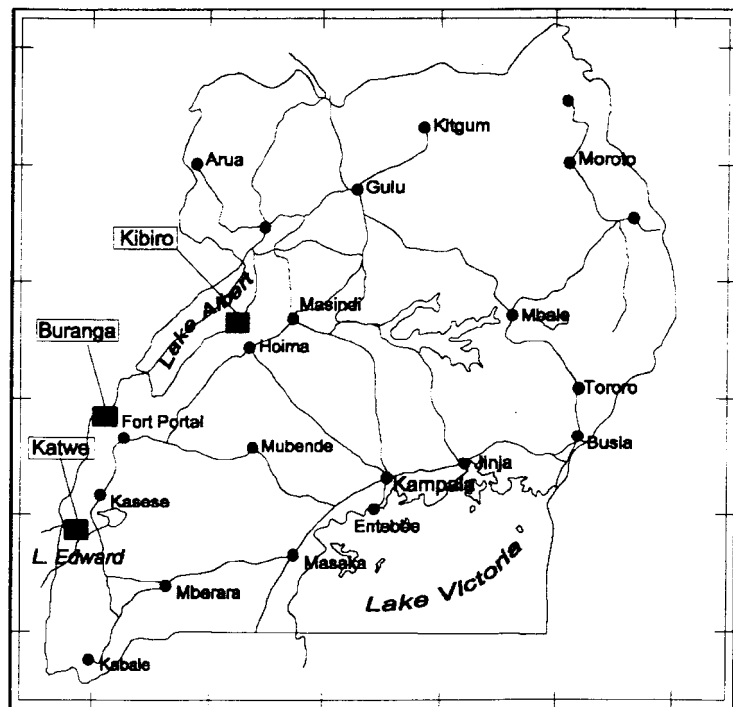


FIGURE 1: Location of study areas in Uganda

According to Ármannsson (1994), geothermal fluids at Katwe rise through sediments and relatively recent volcanics that cover Precambrian rocks. The hydrology of the area is characterised by a number of water-bearing horizons that are, to differing degrees, self-contained. Three types of water occur in the numerous crater lakes in the area: saline, fresh spring and brackish groundwater. Geothermal surface manifestations are found in the saline lakes Kitagata and Katwe with estimated subsurface temperatures of 100-150°C,

possibly as high as 200°C in Lake Kitagata if mixing of hot geothermal fluids with groundwater and lake water is postulated (Ármansson, 1994).

At the Buranga geothermal area, fluids rise through thick sediments and volcanic rocks. According to Ármansson (1994), the fluids are relatively saline and accompanied by a considerable gas flow, mainly carbon dioxide. Extensive travertine deposits occur around the springs whose subsurface temperatures have been estimated at about 120°C (Ármansson, 1994). The area is characterised by major tectonic faults and fissure zones which act as migratory pathways for both meteoric and geothermal waters. The water table is high due to heavy rainfall within the area, hence the geothermal surface manifestations in Buranga.

The Kibiro geothermal area is located within the Albertine rift valley, in which there are tertiary to recent deposits of a total thickness of more than 1200 m (Harris et al., 1956). Arad and Marton (1969) suggested a different origin of the solutes in the Kibiro from that in other geothermal areas, possibly due to extraction of salt from salt rich sediments. A temperature of 54°C has been observed at 600 m depths in a borehole nearby (Petroconsultants, 1971). Two sets of subsurface temperatures were obtained by application of geothermometers that is about 150°C and 200°C. Studies of mixing suggest a hot water component with a temperature of about 200°C (Ármansson, 1994).

2.2 Geology

The geothermal areas in Uganda are located in the western rift of the East African Rift Valley, which is characterised by stretched and fault-broken rocks. Strong volcanic activity, associated with the rift faulting, resulted in depositions of pyroclastics and ultramafic xenoliths on Pre-Cambrian rocks or lacustrine beds. The exposed basement indicates the presence of a sialic basement under the rift floor. The rifting occurred in stages and is broadly influenced by structural geology. The southern part (Rukwa-Nyasa-Urema zone) was formed in Cretaceous times. After this the rifting stopped but started again in Neogene-Quaternary time, involving both the southern and the northern (Tanganyika-Kivu-Semliki-Albert) zones. Active subsidence during the Miocene and the lower Pliocene has led to the forming of a rift graben formation (Logatchev et al., 1972).

Volcanic craters along the course of the western rift valley are associated with the rise of the rift-trench floor. They are arranged in a row, of which each northern member is younger and of shorter duration than the southern ones (Logatchev et al., 1972). The northernmost centre consists of recent volcanic occurrences of strongly under-saturated lavas, which form the volcanic craters and cones of the Toro-Ankole fields (Logatchev et al., 1972). The Toro-Ankole volcanic eruptions began in Upper Pleistocene and stopped about 4,000 years ago. The rift basin and its flanking escarpment blocks at Kibiro are bounded by steeply dipping faults. The escarpment is deeply cut by numerous streams and rivers normally structurally controlled. Fault zones are basic hydrogeological reservoirs and act as migration pathways for both cold and hot water. Hence, the location of most of the active geothermal areas are in places where faults intersect. This region of active and geologically young volcanoes is associated with geothermal resources probably due to more recent underlying intrusions.

2.3 Hydrology of the geothermal areas

2.3.1 Introduction to isotope hydrology

Isotope hydrology is a relatively new scientific discipline that uses natural isotopes that form water molecules (Table 1) as well as man-made molecules to identify the source and track the movement of water both on the surface and underground. These isotopes are ideal tracers because they are integral constituents of the water molecules. In combination with conventional geochemical methods, isotope hydrology helps to scientifically map the groundwater reserves.

TABLE 1: The water isotopes

Isotope	Average natural abundance	Half life
^1H	99.985	Stable
^2H	0.015	Stable
^3H	10^{-15}	12.43 years
^{16}O	99.76	Stable
^{18}O	0.20	Stable

Basic definitions. In order to appreciate the use of isotope hydrology as an exploratory tool, it is necessary to be familiar with the background information of isotopes. Atoms with the same number of electrons and protons, but different numbers of neutrons, are called isotopes. Different isotopes belong to the same element because they have the same number of electrons, and hence behave almost the same in chemical reactions.

Isotope measurement. The absolute abundance of an isotope is difficult to measure with sufficient accuracy and necessary precision for geological application. Therefore, relative differences are measured in terms of internationally accepted standards. The result of such comparison-measurement is the delta (δ) notation for the difference between standard and sample, defined as

$$\delta_{(X)} = [(R_X - R_{st})/R_{st}] \times 10^3$$

where $\delta_{(X)}$ = Delta-value of a sample;
 R_X and R_{st} = Isotopic ratios in sample and reference standard, respectively.

R can be $^2\text{H}/^1\text{H}$ or $^{18}\text{O}/^{16}\text{O}$. The delta-value is expressed in per mill (‰). This results in positive delta values if the sample has more of the heavy isotope than the reference standard, negative delta values if the sample has less of the heavy isotopes than the reference standard. For hydrogen and oxygen in water, the standard most commonly used is Standard mean ocean water (*SMOW*), an average value for the isotopic composition of ocean water (Craig, 1961) or the equivalent *VSMOW* (Vienna-SMOW, IAEA).

Comparison of isotopic ratios in a sample with those in a reference standard is made using equipment called a *mass spectrometer*. The basic concept of the design is to convert the sample quantitatively to a gas from the compound of interest, introduction of the gas into the mass spectrometer, ionisation to produce positively charged species, dispersion of different masses in a magnetic field, impaction of different masses on different collectors and measurement of the difference in the ratios of the heavy to light isotope in the sample gas relative to a reference standard gas. In general, hydrogen is analysed as H_2 and oxygen is analysed as CO_2 .

Isotopic variations arise either from isotopic exchange reactions or from mass-dependent fractionations that accompany physical-chemical processes occurring in nature governed by kinetic theory and the laws of thermodynamics.

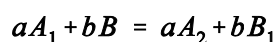
Isotope fractionation. Isotope fractionation is the partial separation of isotopes of the same element during physical or chemical processes. Chemical processes involve breaking bonds. Heavy isotopes form stronger bonds than light ones. Hence, they tend to be concentrated in phases with stronger chemical bonds. There are two different types of isotope fractionation processes: *Kinetic isotope fractionation* which occurs when the rates of processes differ between isotopic species (as a result of molecules with lighter isotope moving faster) and *equilibrium isotope fractionation*, which occurs as a result of differences in thermodynamic properties (bonding properties) of molecules containing different isotopes. Isotopic fractionation between two substances accompanying a specific process is expressed in terms of a fractionation factor, α :

$$\alpha = R_m/R_w$$

where α = Fractionation factor;
 R_m and R_w = Isotopic ratios in rocks and fluid water.

The abundance of the rare isotope is divided by the abundance of the common isotope, so that $R \ll 1$. There is an inverse relationship between the fractionation factor, α , and the temperature, so that fractionation is smaller at higher temperatures, and α becomes equal to 1 (no fractionation) at very high temperatures. How much fractionation occurs depends on the temperature, as well as on the specific atoms involved. The largest differences in behaviour occur for those isotopes that have the largest relative difference in mass. There is a much greater fractionation between hydrogen and deuterium than we see in oxygen, where the difference in mass is only $[(18-16) / 16] = 1/8$.

Isotope exchange reactions. Isotope exchange reactions are equilibrium reactions in which the isotopes of a single element are exchanged between two substances. The chemical composition of reactants and products is the same, but they have different isotopic compositions:



In most surface and near-surface environments, the amount of water is much larger than the amount of the exchanging solid phase, and the isotopic composition of the water is, therefore, not measurably altered on a local scale. The deuterium concentration is almost unchanged because of the generally low abundance of hydrogen in the rocks. However, some exchange of deuterium with hydrous minerals does occur in systems where a large proportion of clay and micaceous minerals occur in the rocks. Where the amount of water is comparable to or less than the amount of rock with which it interacts, the isotopic composition of the water may be substantially altered and this is the basis of using stable isotope technique in hydrologic investigations. At high temperatures, minerals are more susceptible to isotope exchange without obvious chemical alteration than they are at low temperatures, except when a chemical or a mineralogical reaction involving the two phases occurs. Due to water-rock interaction at temperatures greater than 150°C, there is usually an enrichment of $\delta^{18}\text{O}$ to varying extent detected in the thermal waters with hardly any corresponding increase in the $\delta^2\text{H}$ (δD). This $\delta^{18}\text{O}$ enrichment is called oxygen shift.

Application of water isotopes. Water isotopes are generally used in geothermal studies to identify the origin of geothermal fluids and to define the physical and chemical parameters of the geothermal reservoir for optimal exploitation. They can also be applied to monitor geothermal systems, study responses to exploitation and sometimes as geothermometers.

Geothermal waters cool as they rise to the surface and this can occur by conduction, mixing and boiling (Henley et al., 1984). Each of these processes can be traced isotopically. Mixing with cold water before and after boiling is very common in geothermal systems and this can be detected by a change in isotopic composition. Isotopic compositions of mixtures are intermediate between the compositions of the end members. Any mixing proportions of two water sources with known $\delta^{18}\text{O}$ and δD values will fall along a tie line between the compositions of the end members on a $\delta^{18}\text{O}$ and δD plot (Kendall and Caldwell, 1998). If two streams with known discharge (Q_1 , Q_2) and known $\delta^{18}\text{O}$ values ($\delta^{18}\text{O}_1$, $\delta^{18}\text{O}_2$) merge and become well mixed, the $\delta^{18}\text{O}$ of the combined flow (Q_T) can be calculated from

$$Q_T = Q_1 + Q_2 \quad \text{and} \quad \delta^{18}\text{O}_T Q_T = \delta^{18}\text{O}_1 Q_1 + \delta^{18}\text{O}_2 Q_2$$

Extensive boiling in producing aquifers of liquid-dominated reservoirs causes cooling of the flowing fluid. Knowledge of steam-water isotope fractionation can be used to calculate isotopic changes in hot spring water that loses heat by boiling during ascent from the reservoir.

Meteoric lines. A linear relationship between δD and $\delta^{18}O$ for most cold water of meteoric origin has been observed. Friedman (1953) first discovered the covariance between δD and $\delta^{18}O$ values of natural water, comparing his hydrogen isotope data with the oxygen isotope data of Epstein and Mayeda (1953). Craig (1961) published many analyses of both isotopic ratios made on the same samples and defined the now universally recognised 'Meteoric water line' abbreviated as MWL with the expression below:

$$\delta D = 8(\delta^{18}O) + 10$$

The above expression describes the global meteoric water line, and in spite of the complex interactions that occur during the meteoric process, there is a remarkably good worldwide correlation. However, some local meteoric lines have been defined and in the present study, application was made of the Kenyan rain line defined by Clarke et al. (1991) with the expression:

$$\delta D = 5.56(\delta^{18}O) + 2.04$$

Ármansson (1994) defined another line called the Continental African rain line (CARL) defined by the expression:

$$\delta D = 7(\delta^{18}O) + 11$$

The above three lines were applied in this study to define the origin of geothermal fluids and the physical and chemical parameters of the geothermal reservoirs.

2.3.2 The Buranga geothermal area

The Buranga geothermal area (Figure 2) is at the foot of Rwenzori Mountains located in the western rift. The Rwenzori Mountains comprise a host block elevated between faults. The mountains are hidden in cloud cover created periodically by moist air streams from the Atlantic and Indian oceans. The mountains are covered by permanent ice and snow, with a total of 37 small glaciers and ice fields covering about 64 km². The mean annual rainfall reaches up to 2000 mm at an altitude of about 4600 m a.s.l. The Buranga area is generally humid and characterised by excess

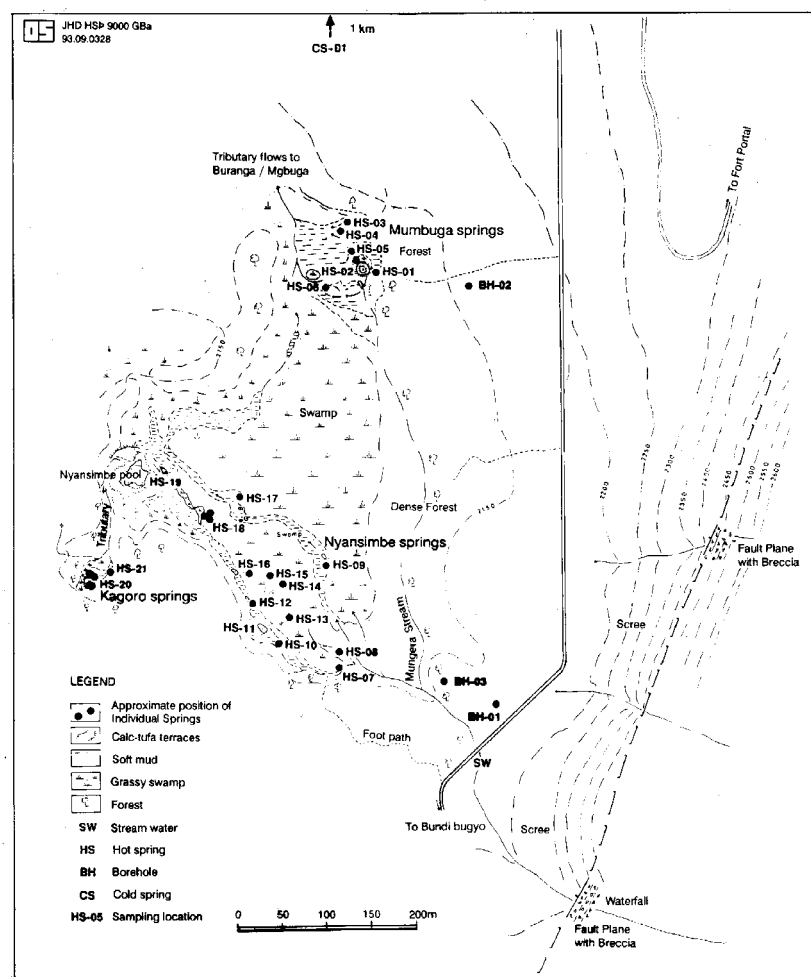


FIGURE 2: Buranga geothermal area sampling locations

moisture because of the excess of precipitation over evaporation. There is a potential of groundwater recharge in the area from snowmelt run-off, small lakes in upper valleys and local precipitation. The area is bounded by major marginal tectonic faults crossed by numerous minor faults in different directions through which drainage takes place. Buranga has the largest surface manifestation, the highest surface temperature and the greatest yield (Ármannsson, 1994) among the three studied areas. The water table is high in this area, with very efficient infiltration in highly permeable, strongly fissured and faulted rocks.

Chemical and isotopic analyses are available for hot spring water, cold stream and spring water samples. The sample locations are shown in Figure 2 and the chemical and isotopic data in Table 1 in the Appendix.

The δD and $\delta^{18}O$ values of hot spring water, cold stream water and spring samples are plotted in Figure 3. The figure demonstrates that the water plots close to the African rain line. The isotopic composition of the cold stream water sample (SW) is -2.24 and -3.7 in $\delta^{18}O$ and δD values, respectively and that of the cold spring water sample (CS-01) is similar although slightly more depleted (-2.57 and -4.6 in $\delta^{18}O$ and δD values, respectively). These waters are believed to represent the local mean precipitation values. The hot spring water samples are more depleted and cluster around -3.5 and -13.4 in $\delta^{18}O$ and δD values, respectively, indicating that the origin of the hot water may be from a higher altitude. It has been suggested that the recharge to the thermal area is from the Rwenzori Mountains (Ármannsson, 1994), but unfortunately no isotopic data are available for high altitude precipitation. However, due to the small difference in isotopic composition of the local cold water and the geothermal water (about 1‰ in $\delta^{18}O$ value) it is suggested that the geothermal water is mostly local in origin slightly mixed with distant high altitude water with lower $\delta^{18}O$ values. No water rock interaction can be detected from isotopic values indicating a shallow low-temperature flow path in agreement with solute geothermometers (Ármannsson, 1994). The homogeneity of the isotopic composition of the Buranga thermal water may indicate that the area has a single hot water reservoir. Geographical distribution of the $\delta^{18}O$ values for water samples does not provide valid information about the preferential flow path in the area.

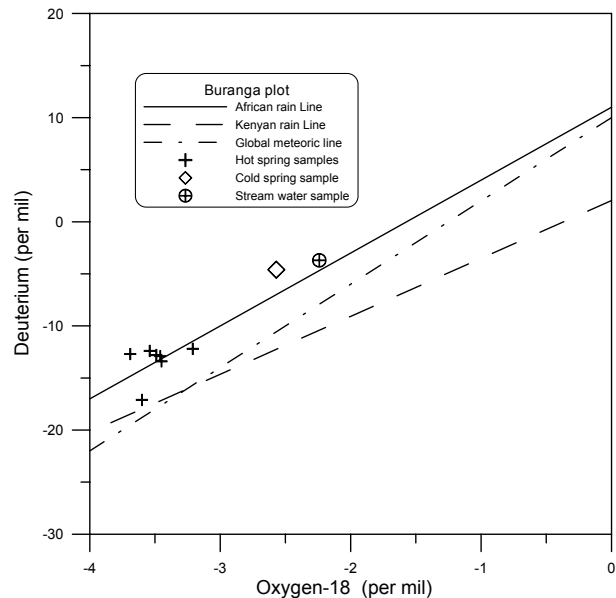


FIGURE 3: $\delta D - \delta^{18}O$ content of hot and cold water samples from the Buranga area

2.3.3 The Katwe-Kikorongo geothermal area

The Katwe-Kikorongo area is hot and dry with mean annual rainfall on the order of 875-1000 mm. It lies at an elevation of 912 m with a mean annual temperature of about 27°C. In some parts at higher altitude, the mean annual rainfall may exceed 1875 mm while barely 10-30 km away in the rift valley, the corresponding rainfall is less than 875 mm (EASD, 1996). The area is characterised by low precipitation and high rates of evaporation with much reduced surface outflow of groundwater. Evaporation exceeds precipitation, and as a consequence salination of the groundwater occurs in the upper layers (salts are precipitated on and near the surface). There are several lakes in the area formed during volcanic explosions. Some of these lakes are hydrologically closed due to lava damming of topographic lows. The area is characterised by lavas, pyroclasts and hydrothermally altered rocks. Meteoric water percolates along fissures and faults to water-bearing layers. Katwe-Kikorongo hydrogeological system is complex and it is difficult to designate independent water-bearing horizons because of rapid changes in the composition and properties of the rocks. Impermeable rocks hinder hydraulic connection with adjacent water-bearing horizons, thus giving the water-bearing strata partly hydrogeochemical individuality.

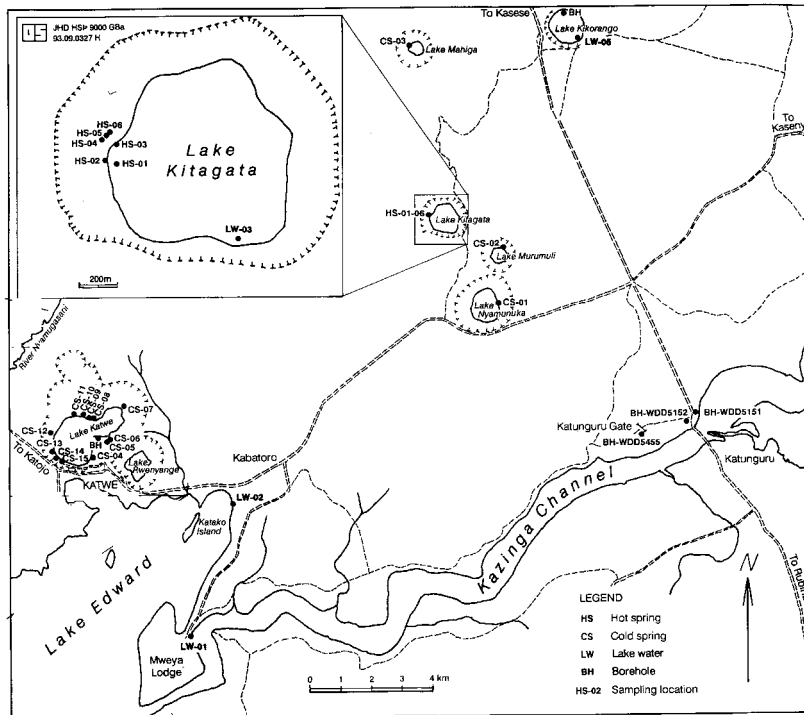


FIGURE 4: The sampling locations within the Katwe-Kikorongo geothermal area

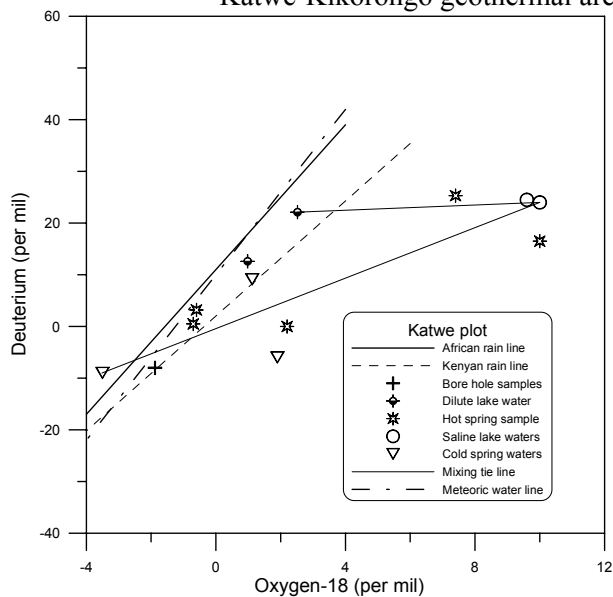


FIGURE 5: δD - $\delta^{18}O$ values for cold and hot water samples from Katwe-Kikorongo area

Chemical and isotopic analyses are available for hot and cold spring water, cold borehole water and some dilute and saline lake samples. The location of sampling points is shown in Figure 4. The salinity of the samples is quite variable as demonstrated in Table 1 in the Appendix.

The isotopic results for the Katwe-Kikorongo water are shown in Table 1 in the Appendix and in Figure 5. Cold spring water samples range from -3.52 to 1.9 in $\delta^{18}O$ values with saline spring water samples having positive values and dilute spring water samples having more negative values, suggesting evaporation in the former.

The isotopic composition of the saline lake samples (around $+10\%$ in $\delta^{18}O$ and around $+24\%$ in δD indicates intense evaporation. The dilute Lake Edward and the Kazinga channel water samples are more depleted than saline lake samples and plot between the African and Kenyan rain lines. Lake Edward is isotopically heavier ($\delta^{18}O = 2.5\%$, $\delta D = 22\%$) than the Kazinga channel ($\delta^{18}O = 0.98$, $\delta D = 12.6$) indicating more evaporation for the former. Both water samples are more enriched than dilute cold groundwater samples (samples CS-13 and BH-5455), which might be their common origin. The isotopic composition of the hot spring samples indicates a mixing between the dilute groundwater and saline Lake Katwe. However, one of the hot spring samples (HS-01) may indicate a mixing between Lake Edward dilute water and Lake Katwe saline water. The geothermal water is of meteoric origin, but has undergone different degrees of evaporation and

mixing. There is no overall preferred isotopic gradient trend in the area. Instead there are several distinct hydrological systems, each with its own hydraulic characteristics according to the geographical distribution of $\delta^{18}O$ value. The high isotopic gradients (Lake Kitagata $\delta^{18}O = -0.73\%$ to $+10.0\%$) are probably related to hydraulic gradients ascribed to the presence of impermeable rocks at the edge of the crater depression. Recharge of subsurface water-bearing systems is likely to be secured by infiltration along fissures and faults along the perimeter of crater depressions.

2.3.4 The Kibiro geothermal area

The Kibiro geothermal area lies on the shores of Lake Albert, in one of the lowest and hottest part of Uganda. Lake Albert was formed by water filling the rift troughs. The area is at the escarpment front in the rift basin about 675 m above sea level. The area is hot (annual temperature 26°C) and dry with mean annual rainfall on the order of 864-1000 mm, characterised by intense evaporation and low humidity. Evaporation exceeds precipitation; as a consequence, salination of the groundwater occurs in the upper layers (salts are precipitated on and near the surface). On the escarpment, the annual rainfall increases rapidly with altitude. There is evidence of tectonic fissuring and faulting in the rocks. Fault zones act as both conductor and accumulator of groundwater against impermeable confining basement rocks. Alluvial materials are presumed to overlie the basement or continental deposits inherited from the rifting stages of development. In Figure 6 the sampling locations are shown for isotopic results reported in Ármannsson (1994), i.e. from Lake Albert, borehole water and hot spring water.

Groundwater samples from boreholes plot close to the Meteoric water line and the African rain line with a range of -3.5‰ to -1.8‰ in $\delta^{18}\text{O}$ values and -15.2‰ to -4.5‰ in δD values as shown in Figure 7 and Table 1 in the Appendix. The heavier values may reflect some evaporation or mixing with some enriched water. The δD values of the thermal springs are close to the borehole values, suggesting a common origin, possibly local precipitation. Their $\delta^{18}\text{O}$ values suggest an oxygen shift of about 1‰. Isotopic results for Lake Albert ($\delta^{18}\text{O} = +5.47\text{‰}$, $\delta\text{D} = 39.8\text{‰}$) are quite distinct from other water in the area and demonstrate isotopic enrichment due to intense evaporation.

This year, new isotopic results were obtained from the IAEA laboratory for samples collected from hot springs, boreholes, a shallow well and two rivers. The sampling locations are shown in Figure 8 and the isotopic results are given in Table 2 in the Appendix and shown in Figure 9.

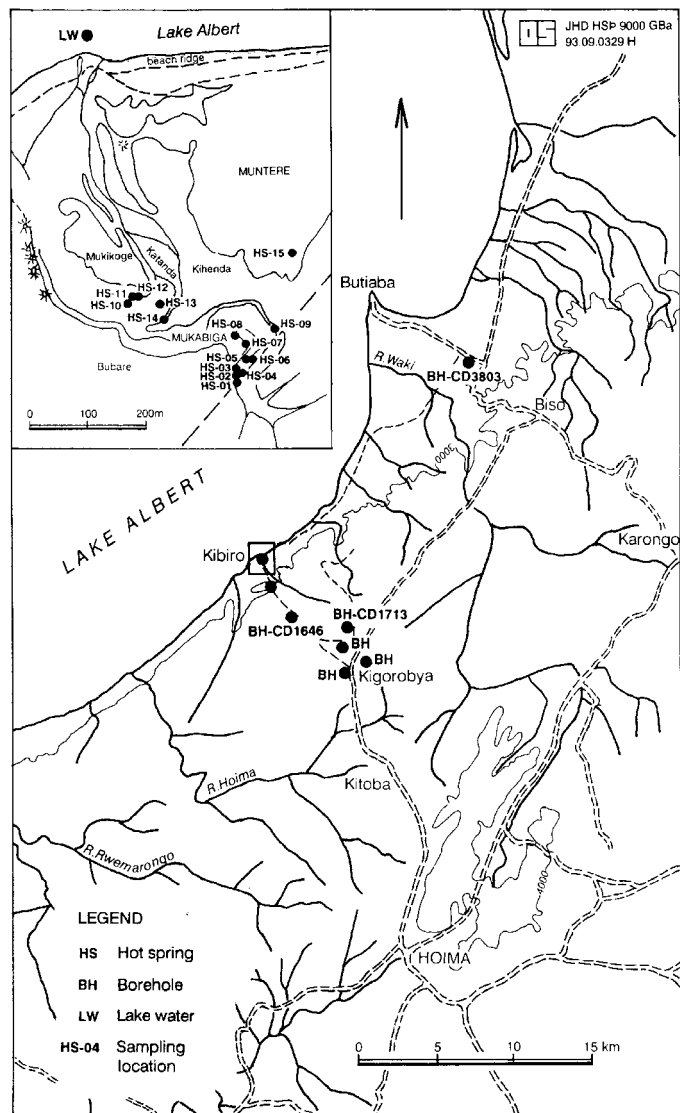


FIGURE 6: Kibiro geothermal area sampling locations (1994-data)

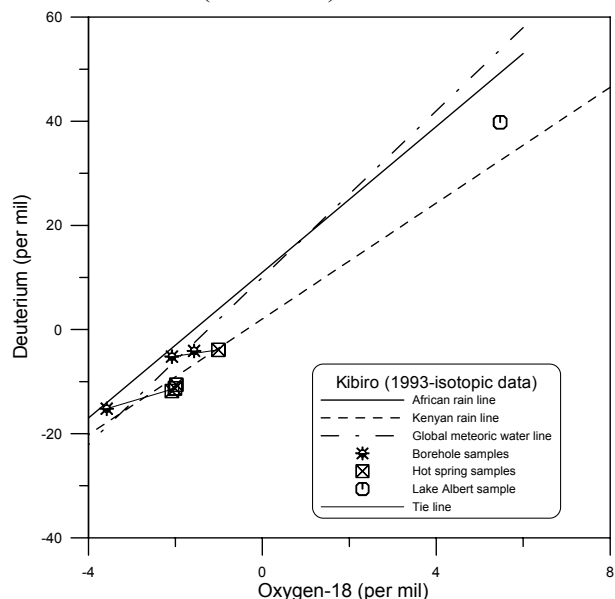


FIGURE 7: δD - $\delta^{18}\text{O}$ values for hot and cold-water samples from Kibiro area (1994-data)

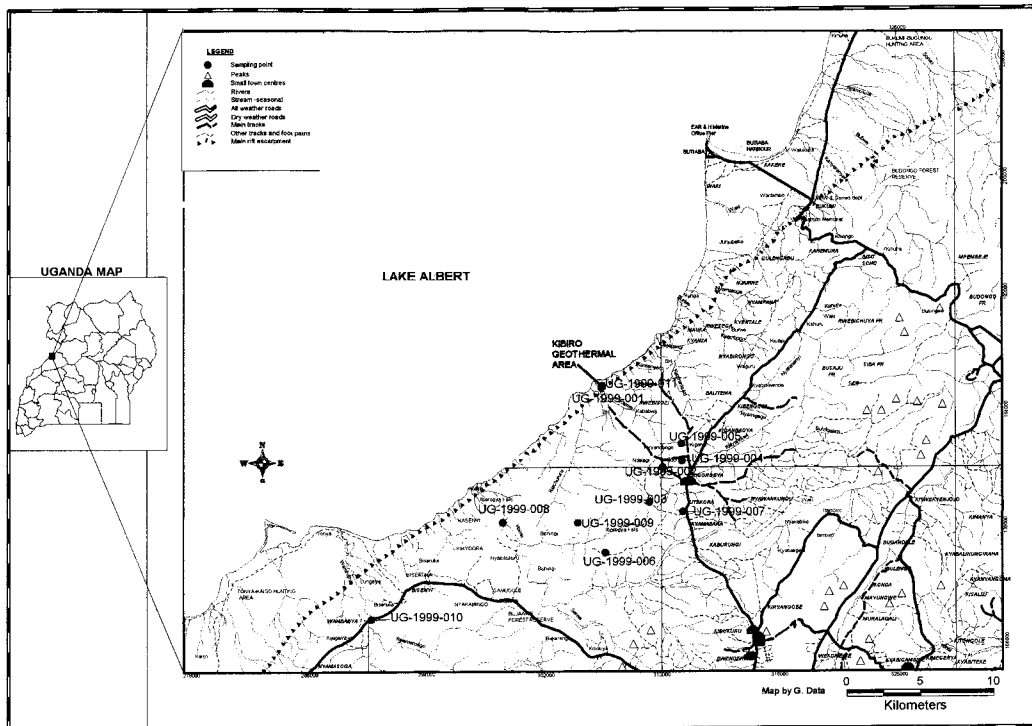


FIGURE 8: Kibiro geological and sampling locations map (2000-data)

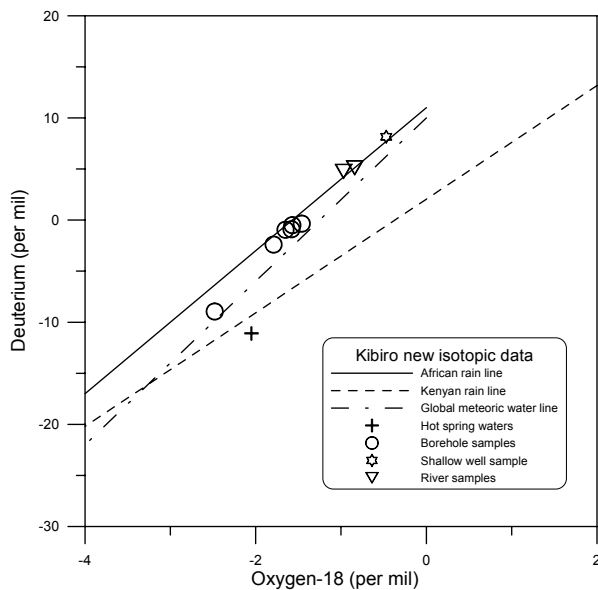


FIGURE 9: δD - $\delta^{18}O$ values for hot and cold water samples at Kibiro geothermal area (2000-data)

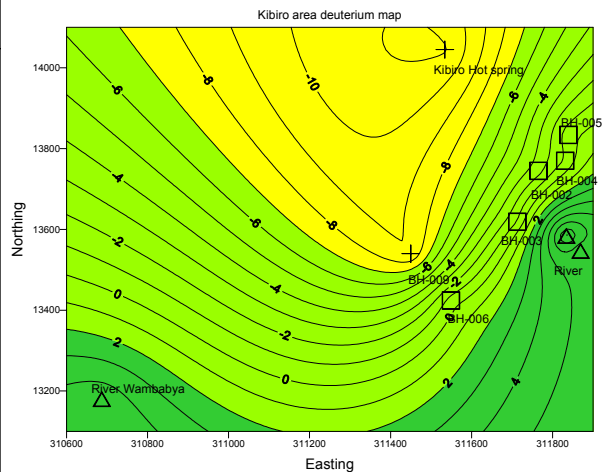


FIGURE 10: Kibiro deuterium map from the 2000-data

The figure shows that the river samples plot on the African rain line with $\delta^{18}O$ values -0.97‰ and -0.84‰ . The corresponding δD values are 4.8‰ and 5.1‰ indicating the same source for the two rivers. The isotopic composition of ground-water that was found in a shallow well is similar although slightly enriched (-0.47‰ and $+8.2\text{‰}$ in $\delta^{18}O$ and δD , respectively). Borehole water samples are more depleted, ranging between -2.2‰ and -1.6‰ in $\delta^{18}O$, falling within the range of borehole samples reported by Ármannsson (1994). The hot spring sample has a very similar δD value to one of the borehole sample (UG-009) suggesting a common origin (Figure 10). A slight oxygen shift (1‰) is observed for the thermal water in agreement with 1994 data. The two data sets, analysed at different laboratories (University of Iceland and IAEA), are consistent and comparable as shown in Figure 11, where the entire data for the Kibiro area is shown.

Geographical distribution of $\delta^{18}\text{O}$ values does not provide valid information about the preferential flow path in the area. Recharge of subsurface water-bearing systems appears to be at the basin margins where water-bearing alluvial deposits emerge at the surface. Tectonic fractures or faults at the margins with a gravitational nature constitute the drainage, hence, are probable recharge zones in this area.

2.4 Chemical characteristics of the geothermal fluids

The chemistry of the three geothermal areas varies mainly due to the geological environments in which they are found. Generally the waters are high in dissolved solids due to high chloride content of the dissolved rocks. The main cations are sodium and potassium with appreciable calcium and magnesium occurrences. The water also contains silica, with neutral to slightly alkaline pH. CO_2 predominates in the gaseous phase of the Buranga area while methane predominates at Kibiro area.

2.4.1 The Buranga geothermal area

The Buranga geothermal fluids are classified as chloride-sulphate-hydrogen carbonate whose composition is probably controlled by volatiles in volcanic rocks (Ármansson, 1994). The total dissolved salts are in the range 14-17000 ppm and plausible solute geothermometers yield relatively constant values in the range of 110-130°C (Ármansson, 1994).

A plot of $\delta^{18}\text{O}$ versus chloride forms two distinct clusters, one of geothermal water samples and another of cold meteoric water samples (Figure 12). The content of dissolved solids is appreciably higher in hot spring water than in cold meteoric water samples, thus indicating intense chemical reactions between water and rock. This could not be inferred by isotopic analysis, probably due to low subsurface temperature since $\delta^{18}\text{O}$ exchange reactions are usually very slow below 200°C.

The geothermal water samples have a high concentration of boron compared to cold stream and spring water samples in the area. The chemical homogeneity of hot spring water may be due to well-mixed water, which is consistent with isotopic derivation. Subsurface temperature was assessed based on the silica content (Fournier and Potter, 1982) and the ratio of sodium to potassium (Ármansson et al., 1983) in the thermal water. Ármansson et al. (1983) gives two Na/K geothermometers. One of them is based on the ratios of the component concentrations (analysed concentrations) of Na and K. The other is based on the ratio of the Na^+ and K^+ activities. These activities may both be reduced significantly by the formation of sulphate complexes (NaSO_4^- and KSO_4^-), when the sulphate concentration in the geothermal water is high. However, both Na^+ and K^+ are not reduced in equal proportions, thus the

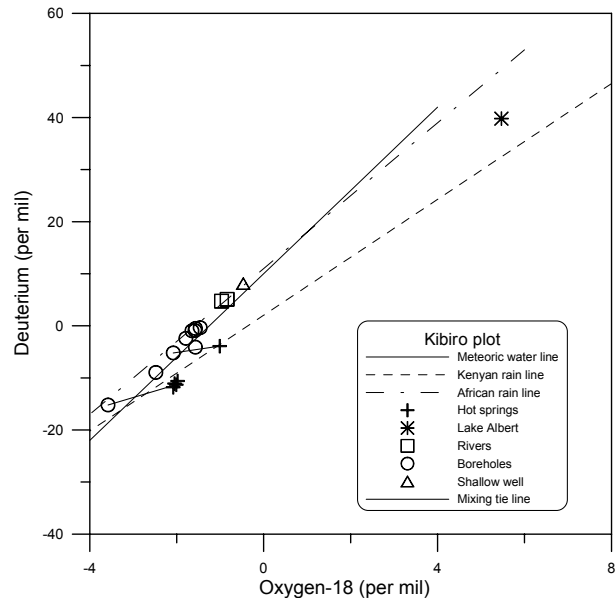


FIGURE 11: The δD - $\delta^{18}\text{O}$ contents of cold and hot water sample data for Kibiro area (entire data)

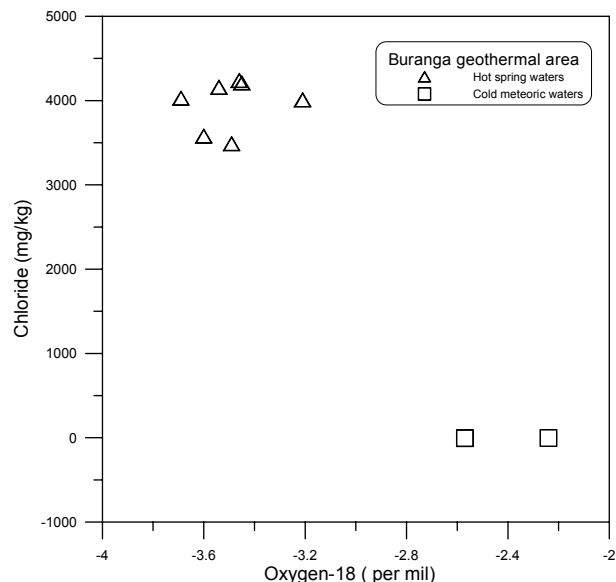


FIGURE 12: Relationship between chloride concentration and $\delta^{18}\text{O}$ values at Buranga

activity concentration ratio of the Na⁺ and K⁺ may differ significantly from the component concentration ratio of Na and K. This causes the Na/K geothermometer to yield different results for fluids with high sulphate concentrations. For the Quartz geothermometer, according to Fournier and Potter (1982), the temperature, T , is given by

$$T = -42.198 + 0.28831c - 3.6686 \times 10^{-4}c^2 + 3.1665 \times 10^{-7}c^3 + 77.034 \log c$$

For the Na/K geothermometer, Arnórsson et al. (1983) calculates temperature, T (°K), as

$$\log Na/K = -1.782 - 2775.5/T - 558780/T^2 - 0.00969T + 4.104 \log T$$

The above equation by Arnórsson et al. (1983) is valid for 25-350°C and is applied in the geochemical program WATCH, (Bjarnason, 1994) which is a tool for interpreting the chemical composition of geothermal fluids. This program reads chemical analyses of samples collected at the surface and computes the properties of aquifer fluids, which include pH, aqueous speciation, and partial pressure of gases, redox potentials and activity products. The program uses activities to compute subsurface temperatures instead of component concentration. The subsurface temperature computed for Buranga is shown in Table 2.

TABLE 2: Chemical geothermometer temperatures for Buranga

Sample no.	T _{quartz} (°C)	T _{Na/K} (°C)
HS-02	114	102
HS-05	121	102
HS-13	128	102
HS-20	124	101
HS-19	119	102
HS-17	103	103
HS-09	116	103

The active hot springs in Buranga provide abundant data on subsurface temperatures based on silica content and the ratio of sodium to potassium in thermal water. The low temperature reservoir indicated may be due to greater meteoric recharge or greater heat conduction due to shallow reservoir depths. The reservoir fluid is close to saturation with calcite. The system probably contains enough water at a high enough temperature to drive a binary condensing turbine.

2.4.2 The Katwe-Kikorongo geothermal area

The geothermal fluids are classified as alkaline sulphate (Ármansson, 1994). Lake Katwe spring water is probably secondary in origin and the geothermal fluids might be sealed off by deposits, with heat and gas escaping to mix with groundwater (Ármansson, 1994). Lake Kitagata geothermometry results are widely scattered and so are the mineral equilibrium temperatures deduced from $\log(Q_m/K_m)$ diagrams (Ármansson, 1994). Secondary converging points below the zero line suggesting mixing with cooler water are observed at approximately 160°C, and mixing models suggest possible mixing with colder water but with a wide scatter in values (Ármansson, 1994).

A plot of $\delta^{18}O$ versus chloride for Katwe water creates a cluster of points separating dilute spring water from saline spring water and saline lake water (Figure 13). The figure shows how the thermal water plots on evaporation or a mixing line between dilute borehole water and saline lake water. Low chloride water relates to local meteoric water while high chloride water relate to geothermal water samples. Decreasing $\delta^{18}O$ is related to decreasing boron content in thermal water. As with isotopic composition, the chemistry

of the geothermal waters at Katwe is not homogeneous. The chloride concentration reaches values up to 20,000 mg/kg indicating a potential to cause considerable deposition-related problems. High temperature deep-water circulation is indicated by high silica and low calcium values in samples with high boron values. Chloride-sulphate ratios are higher in the Katwe saline lake than in other places indicating a possible deep-water component. High temperatures are also reflected in low Na/K ratios in samples. The total dissolved solids (TDS) and sulphate in geothermal water is about 100 times that in lake water. The content of dissolved solids such as, for instance, silica and chloride is appreciably higher than in cold water, thus indicating more intense chemical reactions between water and rock. Silica and sodium have increased almost ten times in geothermal water.

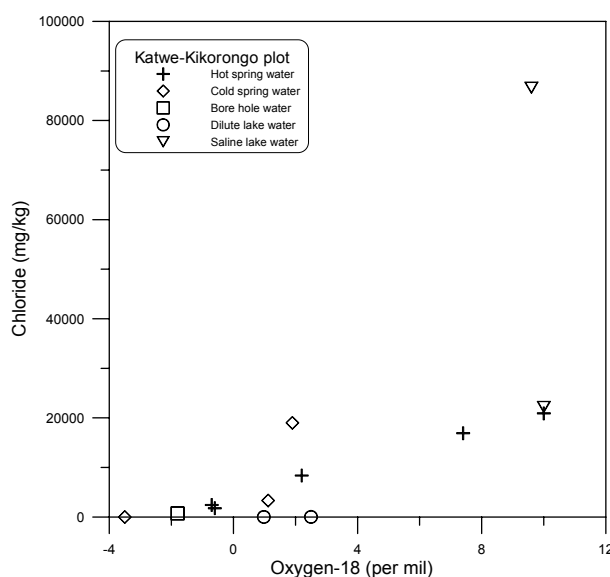


FIGURE 13: $\delta^{18}\text{O}$ value versus chloride concentration in mg/kg at Katwe-Kikorongo

The wide range of values for subsurface temperature in Katwe-Kikorongo reflects the complexity of this system (Table 3). According to the calculated temperature by geothermometers, Katwe-Kikorongo appears to be a moderate- to high-temperature hydrothermal system, from which electricity might be produced.

TABLE 3: Chemical geothermometry temperature for Katwe-Kikorongo

Sample no.	T_{quartz} (°C)	$T_{\text{Na/K}}$ (°C)
HS-05	112	140
HS-02	120	155
HS-01	89	113
HS-01	86	116
HS-01	38	111

2.4.3 The Kibiro geothermal area

Kibiro geothermal fluids are classified as alkali chloride water according to Ármannsson (1994). A model was constructed which entails 70% geothermal component (200°C), 16% brackish groundwater and 14% fresh groundwater. Mixing models suggest that there is no boiling in the system and that the temperature of the geothermal component is 190-220°C (Ármannsson, 1994). Mineral equilibrium diagrams give a temperature range of 140-160°C, and the intersection of curves below the zero line at approximately 200°C are compatible with the mixing of geothermal fluids with cooler water (Ármannsson, 1994).

Chloride/sulphate ratios are higher for saline geothermal water than local cold streams and springs, probably due to surface oxidation of sulphides and to low solubility of sulphate minerals at higher temperatures. Generally, geothermal water has higher concentrations of dissolved solids than cold water, thus indicating more intense chemical reactions between water and rock at higher temperatures. The TDS in Kibiro thermal water are about ten times that in the neighbouring lake water. The chemistry of Lake Albert water is quite distinct from that of geothermal water. Silica is almost 250 times higher in hot spring water than in Lake Albert water. Sodium is about 20 times higher in geothermal water than in lake water while chlorine has increased about 100 times in the geothermal water. The $\delta^{18}\text{O}$ -chloride plot shows a

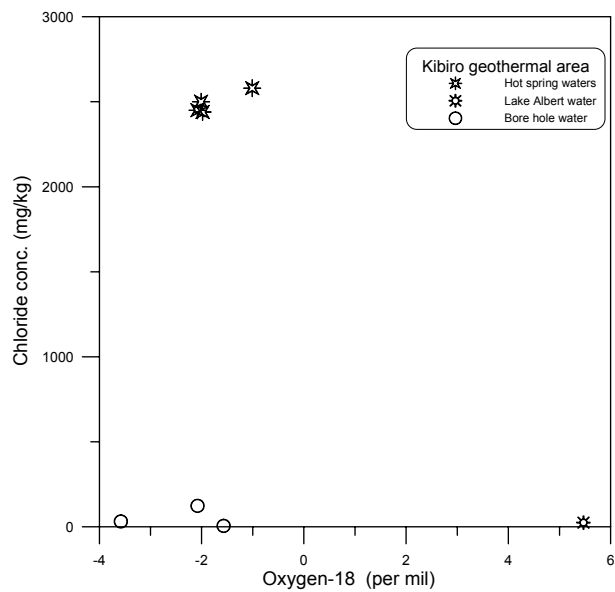


FIGURE 14: Classification of Kibiro water into Lake Albert water, borehole water and hot spring water

non-linear correlation forming clusters of fresh borehole water, lake water and hot spring water (Figure 14).

The Kibiro hydrothermal system, of about 210°C (Table 4), is capable of producing a steam pressure to drive turbine generators. The chemical geothermometer temperature results must be regarded as only a first step in the investigation. The results computed differ slightly from those by Ármannsson (1994) because the WATCH program computes subsurface temperature based on activities that are affected by a high concentration of sulphate ions while Ármannsson (1994) based his calculation on component or analysed concentrations.

TABLE 4: Chemical geothermometer temperature for Kibiro

Sample no.	T _{quartz} (°C)	T _{Na/K} (°C)
HS-02	149	211
HS-05	147	211
HS-14	146	213
HS-17	149	216

2.5. Conclusions

Buranga

- The $\delta^{18}\text{O}$ and δD values of the geothermal water are lower than those of the local spring and stream water, indicating that their origin is at a higher altitude than the cold water. Cold streams and springs in high altitude areas surrounding the geothermal area should be sampled to determine their isotopic composition.
- The $\delta^{18}\text{O}$ and δD values of stream and spring water may represent the average annual composition of meteoric water in the area.
- The constancy of $\delta^{18}\text{O}$ values suggests a single well-mixed geothermal reservoir probably fed from a single source.
- The local meteoric water seems to infiltrate to depth through fault and fissures, becoming heated and rising again. Tectonic structures, mainly fault systems in the area should be mapped thoroughly as they are the most probable migration pathways in the area.

Katwe-Kikorongo

- Katwe-Kikorongo geothermal area is recharged from a mixture of cold dilute groundwater and saline lake water.
- High $\delta^{18}\text{O}$ gradients correspond to high hydraulic gradients that can be explained by the presence of impermeable rocks which limit the mixing effects at short distance.
- Lake Edward water might be involved in the recharge of hot spring water as inferred by a possible tie line between dilute and saline lake water.
- $\delta^{18}\text{O}$ enrichment gradients differ from zone to zone in Katwe-Kikorongo geothermal area with no

identifiable preferential flow path in this area. This is explained by several independent distinct groundwater systems due to impermeable barriers.

- The isotopically heavier water at Katwe-Kikorongo approaching the $\delta^{18}\text{O}$ value similar to magmatic or metamorphic water ($\delta^{18}\text{O} = +10\text{‰}$) can be explained by intense evaporation.

Kibiro

- Very good agreement is observed for the two data sets (from 1994 and 2000) available for the isotopic composition of the water within the Kibiro area. It is suggested that the thermal water at Kibiro and the cold groundwater have a common origin, possibly local precipitation, and oxygen shift of about 1‰ is observed for the thermal water.
- Lake Albert isotopic composition is quite distinct from that of the hot spring water ruling out the possibility of direct recharge by the lake water, despite its close proximity.
- River samples have similar δD -values to the lake suggesting a common source. Their values are, however, very different from the hot spring δD values, ruling out their direct involvement in the recharge of the geothermal systems.
- The geology of the recharge areas in Kibiro consists of crystalline rocks, which are poor aquifers, hence replenishment of subsurface water-bearing systems is likely to be secured by infiltration of local meteoric waters along tectonic fissures and faults. Meteoric water circulates to depth, becomes heated and rises again through a system of faults. Water-bearing fracture zones should be thoroughly studied in these areas.

3. A REVIEW OF ISOTOPIC MONITORING STUDIES IN THE SVARTSENGI GEOTHERMAL FIELD, ICELAND

3.1 Introduction

Three high-temperature geothermal fields, Svartsengi, Eldvorp and Reykjanes are situated on the outer parts of the Reykjanes Peninsula in SW Iceland. The Eldvorp geothermal field west of Svartsengi has not been utilised, but is connected to the Svartsengi field (Björnsson and Steingrímsson, 1991, Eysteinnsson et al., 1993). The Svartsengi field is part of an active fissure swarm, lined with crater-rows and open faults showing only limited signs of surface geothermal manifestations.

In January 1973, Orkustofnun (National Energy Authority) completed its preliminary plans for a geothermal plant in the Svartsengi area. The results of these plans encouraged further research, which the authority undertook for the entire area. Two wells were drilled, 1713 and 1519 m deep, and a resistivity survey was made to ascertain the size of the geothermal area (Georgsson, 1981). By 1993, a total of 14 wells had been drilled in the Svartsengi area, totalling 13.6 km in depth, the deepest one being about 2000 m. Due to the high salinity, heavy scaling and temperature of the geothermal fluids (235-243°C), a method of heat exchange was developed to facilitate the direct utilisation of the geothermal power (Björnsson and Albertsson, 1985).

As a result of production and withdrawal of geothermal fluids over time (1975-1992) in excess of the inflow, there was a progressive decline in reservoir fluid pressure (Björnsson and Albertsson, 1985). This pressure drawdown resulted in land subsidence and expansion of the two-phase boiling zone in the easternmost part of the Svartsengi drilling area, where three wells now yield dry steam. The boiling phase may have led to a reduction in drawdown rates and pressure stabilisation since 1990. Observation of reservoir temperatures, during and after injections of cold fluids, indicates a rapid migration of injected fluids between wells, reflecting the double porosity nature of the reservoir (Björnsson and Steingrímsson, 1992).

Fluid extraction and the subsequent pressure drawdown in Svartsengi have been monitored since the

beginning of production on 18th October 1976. The drawdown was originally measured as water level in a monitoring well, but at present the pressure at depth in well 7 is monitored regularly. The present study is a review of earlier isotopic work done on the monitoring of Svartsengi geothermal field (Bjarnason, 1988, 1996). The variation in the isotopic composition of geothermal fluids over time, as a result of production of reservoir fluids and injection of fresh water, is reviewed. The chemical composition in some producing wells has displayed the effects of dilution by injected fluids.

3.2 Geology of the Svartsengi field

The Svartsengi high-temperature reservoir is among geothermal fields associated with an active rift zone, which is the landward extension of the Mid-Atlantic ridge on the Reykjanes peninsula (Figure 15). The geology is characterised by basaltic lavas at the surface, followed by sequences of lava flows and hyaloclastite, reflecting interglacial and glacial periods (Franzson, 1983; Pullinger, 1991). At a depth greater than 800 m, intrusives become a dominant formation. Intrusives are believed to have intruded horizontally in the depth interval 1100-1300 m. The average reservoir permeability is in the range 100-150 mD (Kjaran et al., 1979). One of the characteristics of the Svartsengi reservoir is an almost uniform pressure distribution in the well field (Björnsson and Steingrímsson, 1992). The reservoir aquifers are predominantly controlled by intrusives and tectonic fractures and faults. The formation of cap rock is evident between 300 and 500 m depths and is attributed to the filling of pore space by alteration minerals and the absence of intrusives. The alteration pattern can be subdivided into distinct episodes where low-temperature conditions are seen to have prevailed prior to high-temperature conditions. Two distinct episodes of high-temperature activity are observed, the latter rises separately to higher elevation. The dominant alteration pattern conforms reasonably well to the present thermal regime in the field (Franzson, 1983).

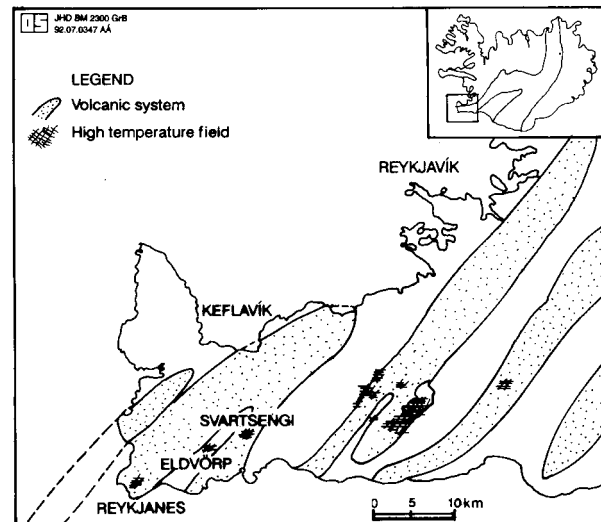


FIGURE 15: The geology and location of the Svartsengi geothermal field

3.3 Characteristics of the Svartsengi field

3.3.1 Hydrology

The Svartsengi geothermal field consists stratigraphically of a shallow groundwater zone in basaltic formations down to 300 m depth. Studies of the hydrology of the area, which is close to the ocean, reveal a fresh water lens of meteoric origin floating on seawater (Ingimarsson et al., 1978). Seawater with concentrations in mg/l with respect to chloride, sodium and silica of 18,800, 10,560 and 0.7, respectively, dominates the chemistry of Svartsengi geothermal fluids which has concentrations of 12,700, 6,500, 410 mg/l, respectively, (Bjarnason, 1995). Fresh meteoric water and seawater feed the geothermal system, resulting in a reservoir fluid of 2/3 seawater and 1/3 freshwater with a uniform temperature of 235-240°C. The geothermal fluid has undergone ion exchange with rocks losing Na, Mg, and SO₄ and gaining Ca, K and SiO₂ (Arnórsson, 1978). The chemical composition of the brines produced is spatially and temporally uniform, suggesting good fluid mixing within the reservoir. The temperature profile below 400-600 m depth is also uniform, again indicating good fluid mixing within the system. A fissure swarm crosses the

reservoir in the eastern part of the well field where fluids discharge to the surface in the form of steaming fumaroles. According to Kjaran et al. (1980) the hydrologic reservoir mechanism is the following, in meteoric water percolates approximately 3 km down from the infiltration area near lake Kleifarvatn and flows westward along the seismic zone, a permeable channel created by regular tectonic movement. This flow picks up heat from the deeper rock formations and mixes with the intrusive cold seawater, forming a saline geothermal fluid. Convection occurs in regions where fissure swarms intersect the seismic zone resulting in the rising of hot fluids which are capped by an impermeable layer at about 600 m below the surface. Some aspects of this model are considered speculative, however.

3.3.2 Utilisation

The Svartsengi field has been utilised by the Sudurnes regional heating company to provide district-heating service to the local communities. The two-phase mixtures produced by the wells are piped to the power plant and used in a heat exchange process to produce hot water. This is done by heating and degassing fresh cold water. Some electric power is also generated. Thórhallsson (1979), Gudmundsson (1983a) and Pálmason et al. (1983) have discussed the power plant and field development. The locations of the 15 geothermal wells drilled in the Svartsengi field are shown in Figure 16.

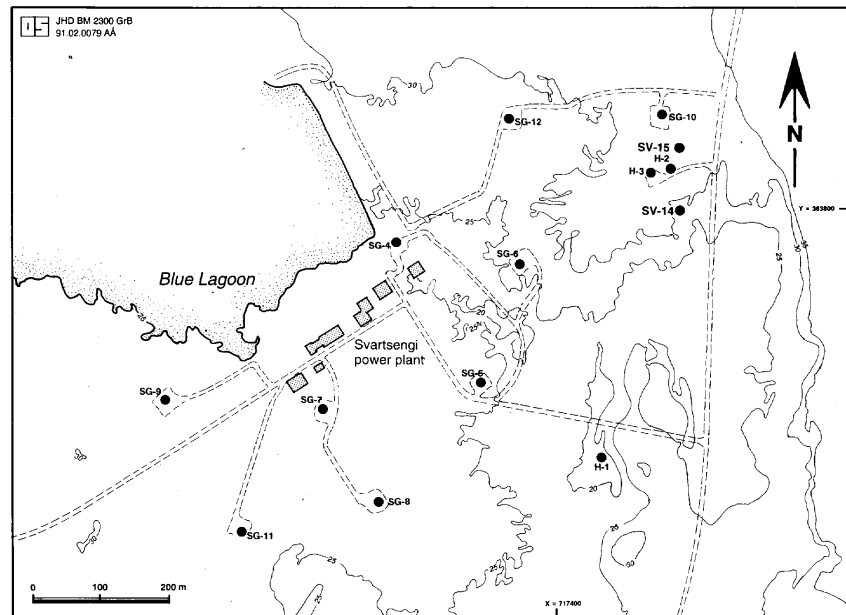


FIGURE 16: Location of wells in the Svartsengi geothermal field (Björnsson and Steingrímsson, 1991)

The locations of the 15 geothermal wells drilled in the Svartsengi field are shown in Figure 16.

Wells H-2, H-3 and SG-10 are 239, 402 and 424 m deep, respectively. Wells SG-4, SG-5 and SG-6 are 1713, 1579 and 1734 m deep, respectively. Wells SG-7, SG-8, SG-9, SG-11 and SG-12 are 1438, 1603, 994, 1141 and 1488 m deep, respectively.

3.3.3 Injection tests

From the start of production, all spent fluids were disposed of at the surface. The spent geothermal brine is supersaturated with silica, which precipitates in a disposal pond by the power plant (Gudmundsson, 1983b). Environmental regulations combined with the need to support the reservoir pressures led to re-injection of a mixture of cooled, condensed steam and spent geothermal brine back into the reservoir. Limited injection tests of fresh water were first carried out in 1982 (Gudmundsson, 1983c and Gudmundsson et al., 1984) to study its effects. Fresh water injection was resumed at the end of 1984 and continued to mid 1988. Spent brine was injected for a while in 1984. Freshwater injection into well SG-12 caused some cooling and fluid dilution in nearby production well SG-6. The cooling effect in well SG-6, which is located 200 m to the south of well 12, reached a maximum of 8°C in 1989.

3.4 Isotopic analysis

Isotopic and geochemical data from wells, temporal trends, interpretations and further documentation on sample acquisition are contained in reports OS-88001/JHD-01 and OS-96082/JHD-10 (see Table 3 in Appendix) by Bjarnason (1988, 1996). A review is given on the isotopic trends in the Svartsengi geochemical data set.

3.4.1 Data processing

In order to calculate the isotopic composition of the total well discharge it is necessary to collect both water and steam at a measured separation pressure, and calculate steam fraction of the discharge from knowledge of well discharge enthalpy. Assuming mass and heat of the fluid ascending are conserved, the heat content of the total well discharge and its composition are the same as those of the water entering the well. In thermodynamics, the well is regarded as an isolated system and for conservation of heat (enthalpy) we have:

$$h^d = h_l^s y_l + h_l^w (1 - y_l)$$

And for the mass component:

$$m_{il}^d = m_{il}^s y_l + m_{il}^w (1 - y_l)$$

h^d stands for enthalpy of the water entering the well, that is, the total enthalpy of the system. h_l^s and h_l^w represent enthalpy of the steam and water, respectively, at a particular pressure P_l . y_l is the steam fraction at that pressure and $1 - y_l$ is the water fraction. The enthalpy of saturated steam (steam in equilibrium with water) is equal to the enthalpy of boiling water plus the latent heat of vaporisation, l , in kJ/kg, or

$$h_l^s = h_l^w + l_l$$

Re-arranging the equations yields

$$y_l = (h^d - h_l^w) / l_l$$

The concentration, c , of any component, including heat and isotope, may be written,

$$c_{reservoir} = (1 - y)c_l + y c_v$$

l and v refer to flashed water and steam phase, respectively, and y to the steam fraction.

3.4.2 Local meteoric line

In Iceland the $\delta^{18}\text{O}$ - δD relationship of the cold groundwater has been defined as $\delta\text{D} = 6.5 \delta^{18}\text{O} - 3.5$, when $\delta^{18}\text{O} \geq -10.5\text{‰}$ and as $\delta\text{D} = 8 \delta^{18}\text{O} + 11$ for lighter precipitation (Sveinbjörnsdóttir et al., 1995). The correlation coefficient is 0.97 for both lines. The $\delta\text{D} = 6.5 \delta^{18}\text{O} - 3.5$ local meteoric water line was used as a reference for interpreting the provenance of Svartsengi geothermal water.

3.4.3 Origin of geothermal waters

The δD - $\delta^{18}O$ relationship between seawater, fresh meteoric water and geothermal water for Svartsengi field is shown in Figure 17. The figure shows that the oxygen and hydrogen compositions of local precipitation are close to -8.0‰ and -55.0‰ , respectively and seawater off the Reykjanes peninsula $+0.2\text{‰}$ and -2.2‰ , respectively. The geothermal water at Svartsengi is $2/3$ seawater and $1/3$ freshwater according to chemical analyses. Thus based on the above numbers, one would expect the isotopic composition of the thermal water to be:

For $\delta^{18}O$: $2/3(+0.2\text{‰}) + 1/3(-8\text{‰}) = -2.53\text{‰}$

and for δD : $2/3(-2.2\text{‰}) + 1/3(-55\text{‰}) = -19.5\text{‰}$

In comparison with the above numbers, the geothermal water is enriched by about 0.5‰ in $\delta^{18}O$ and depleted by about 5‰ in δD . It is suggested that the enrichment in $\delta^{18}O$ values can be explained by an oxygen shift due to hot temperature exchange reactions between the thermal fluid and the subsurface rocks (see e.g. Muehlenbachs and Clayton, 1976). The depletion in δD may reflect previous stage when the circulating fluid was more meteoric than it is today possibly during past glaciations, as has been suggested for the nearby Reykjanes geothermal field (Sveinbjörnsdóttir et al., 1986). At that time the local precipitation on Reykjanes was lighter than at present due to colder climate. In Iceland isotopically light groundwater from that time has been detected in several places (Arnórsson et al., 1993; Sveinbjörnsdóttir et al., 1995) and it is therefore possible that the light nature of the δD values at Svartsengi can be explained by “iceage water” still circulating in the system. This would not be seen in the corresponding $\delta^{18}O$ values due to the observed oxygen shift. The depletion in δD could also be attributed to isotopic exchange with hydrous minerals formed when the fluid was more dilute than today, as suggested by Kristmannsdóttir and Matsubaya (1995). There is no clear relationship between isotope content and chloride concentration of geothermal water. This lack of relationship might be attributed to the interaction of seawater and the hosting rocks, which influence the isotopic composition more than the chloride concentration.

3.4.4 Geographical distribution of $\delta^{18}O$

In 1989, the $\delta^{18}O$ values from well discharges increased progressively in the southwest direction with lowest values detected in well SG-12 and SG-6, with slightly higher values in wells SG-11 and SG-9 (Figure 18). This has been attributed to the injection of freshwater into well SG-12, during the years 1984 to 1988, which was much lower in $\delta^{18}O$ and δD values than the thermal fluids. The same trend was depicted in 1991 with a progressive increase in $\delta^{18}O$ in the southwest direction. In 1992 the field had almost a constant $\delta^{18}O$ value (-1.5‰). In 1993, $\delta^{18}O$ geospatial distribution shows Well SG-12 having the most negative values and well SG-7 being most enriched. In 1994, the reverse trend is observed with $\delta^{18}O$ enrichment in the northeast towards well SG-12 as indicated in Figure 19. The change may be explained by boiling of water in the formation nearby, which would have created an isotopically heavy residual geothermal fluid.

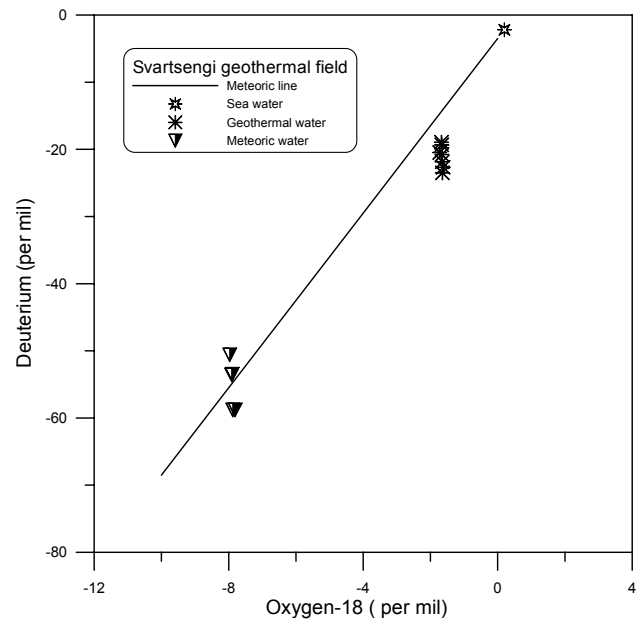


FIGURE 17: Relationship between local meteoric water, geothermal water at Svartsengi and seawater, off the Reykjanes peninsula

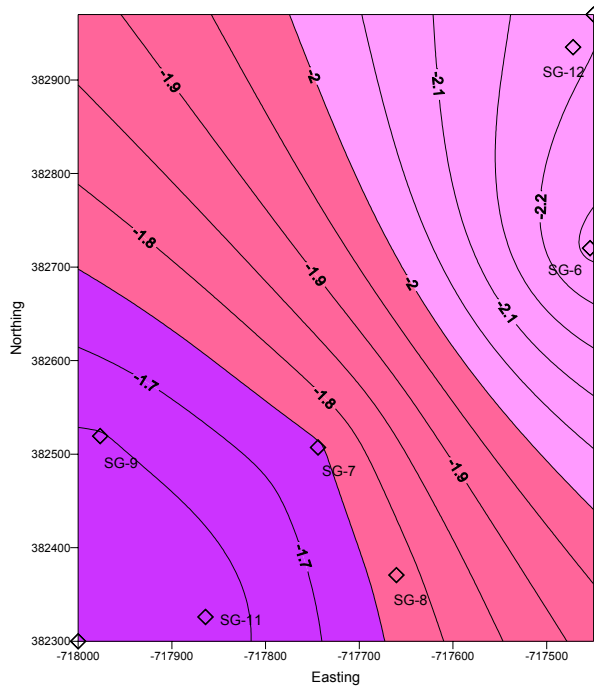


FIGURE 18: The progressive increase in $\delta^{18}\text{O}$ values in the southwest direction in Svartsengi in 1989

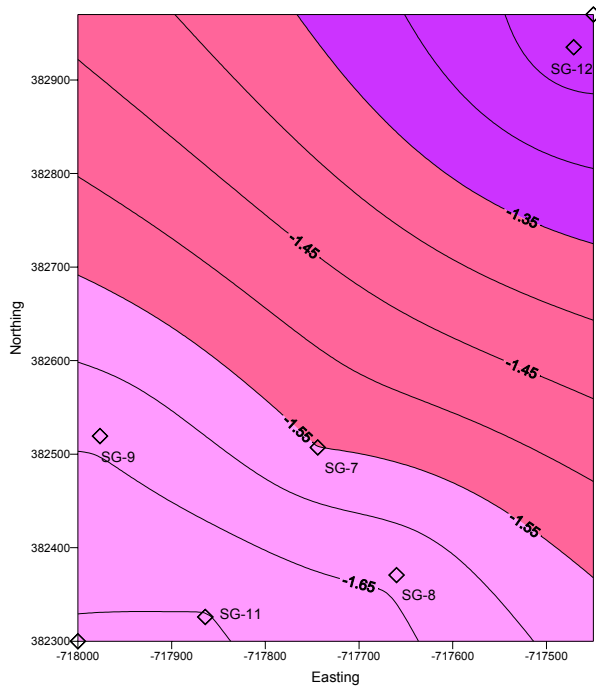


FIGURE 19: The progressive increase in $\delta^{18}\text{O}$ values in a northeast direction in Svartsengi in 1994

3.4.5 Effects of injection (wells SG-6 and SG-12)

As seen in Figure 20, the $\delta^{18}\text{O}$ values in well SG-6 decreased considerably from 1980 to 1987 accompanied by a decrease in chloride concentration. This has been attributed to the diluting influence of freshwater injected into the nearby well SG-12. The $\delta^{18}\text{O}$ values increased from 1988 onwards after injection ceased in 1988. The isotopic enrichment in well SG-12 in 1994 may be ascribed to progressive boiling of water in the aquifer that might have created isotopically heavy residual geothermal water.

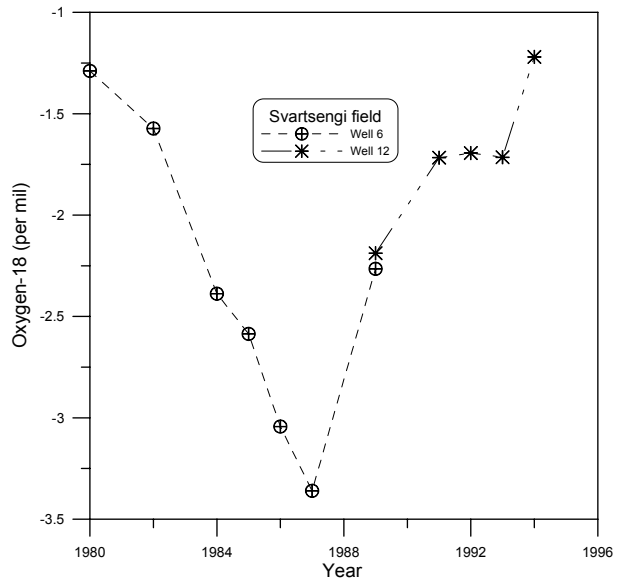


FIGURE 20: The injection effects of well 12 on well 6

3.4.6 Temporal changes in the southwest part of the field (wells 7, 8, 9 and 11)

Information on the temporal variability of the isotopic composition in the southwest part of the Svartsengi geothermal field is shown in Figure 21. There is generally no significant variation in the $\delta^{18}\text{O}$ values in well discharges from 1980 to 1994, besides depletions in 1984 and a slight enrichment in 1985. The depletion in Well SG-11 in 1984 was probably due to a decrease in reservoir pressures that might have caused a steam gain due to boiling. Figure 21 also demonstrates clearly the homogeneity of $\delta^{18}\text{O}$ values in 1992.

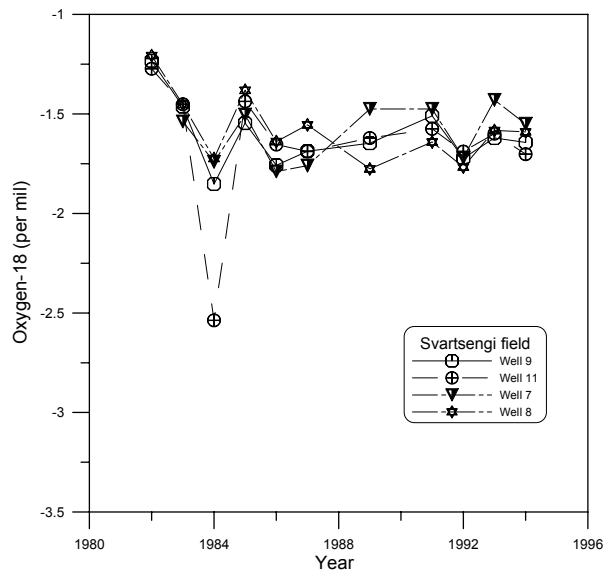


FIGURE 21: Temporal variation of $\delta^{18}\text{O}$ in wells at Svartsengi geothermal field

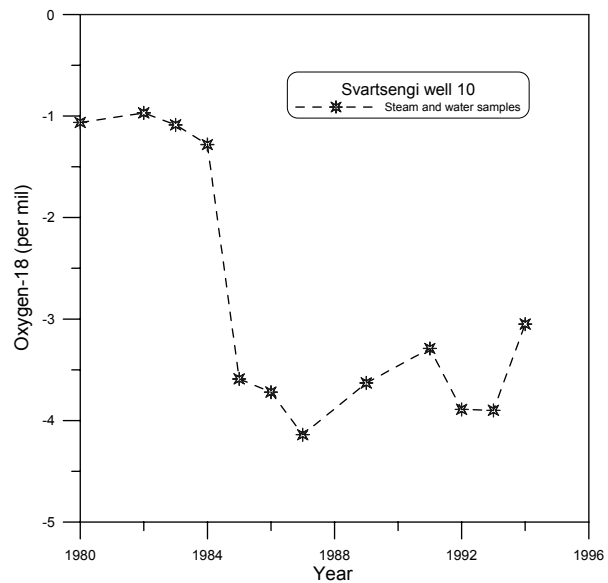


FIGURE 22: $\delta^{18}\text{O}$ variation with time, well SG-10, Svartsengi

3.4.7 Well SG-10

SG-10 was a two-phase well until 1984 when it started to produce dry steam exclusively. The production of dry steam in well SG-10 could be attributed to the reduction of the reservoir liquid level consistent with the progressively lower reservoir pressures observed as a result of production and withdrawal of reservoir fluids over time. The isotopic composition of steam samples is more depleted than that of water samples due to evaporative enrichment of geothermal water and subsequent depletion of the evaporated steam. The temporal changes of $\delta^{18}\text{O}$ values in well SG-10 discern a sharp decline around 1984 (Figure 22) attributed to an exclusively dry steam discharge from this well since April 1984 (Bjarnason, 1988). Slight declines in 1984 and 1992 are probably attributed to steam gain due to enthalpy changes.

3.5 Chemistry of the Svartsengi fluids

The geothermal fluid in Svartsengi is brine at 240°C , consisting of $2/3$ seawater and $1/3$ fresh water. The mixture has undergone ion exchange with the rocks, subsequently losing sodium, magnesium and sulphate and gaining calcium, potassium and silica. The concentration of silica always increases with increasing temperature while the solubility of calcium sulphate and many magnesium salts, in particular magnesium silicates, decreases with rising temperature. On heating with the rock, seawater thus loses magnesium and sulphate (Arnórsson, 1978). Svartsengi geothermal field has been slowly degassing and because of drawdown, well SG-10 has discharged only dry steam since 1984.

In general *chloride* concentrations exhibit no significant variation with time in the Svartsengi geothermal field as demonstrated in Figure 23a. However, slight changes can be noted particularly in well SG-11, probably related to the steam gain in the discharge that might have been caused by boiling. *Boron* concentration does not vary significantly except for a few slight declines (Figure 23b). The variation in 1984-1985 is attributed to different analytical methodologies (Bjarnason, personal communication) while that in 1994 might be due to boiling and subsequent steam gain in the discharge.

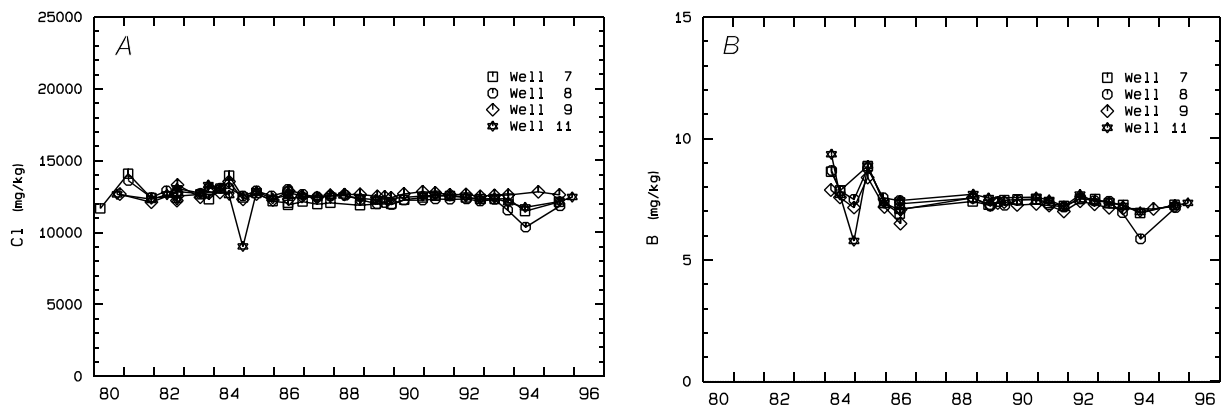


FIGURE 23: Temporal variation of A) chloride and B) boron in geothermal fluids of wells 7, 8, 9 and 11 at Svartsengi geothermal field (Bjarnason, 1996)

Carbon dioxide concentration in production wells varied as seen in Figure 24a, where a broad decline in the 1980's can be detected. The decrease in CO_2 concentration is attributed to progressive boiling in the reservoir that leads to increased loss of CO_2 over time. The increase in wells 11 and 7 after 1989 may be due to an increased contribution of fluids from the deep reservoir. *Hydrogen sulphide* concentration was almost constant with no significant variation, as shown in Figure 24b.

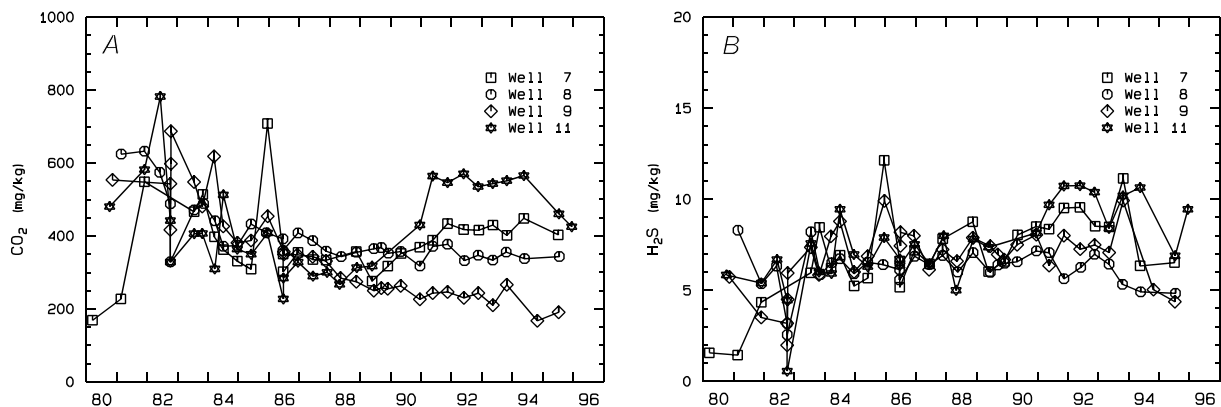


FIGURE 24: Temporal variation of A) CO_2 and B) H_2S from wells 7, 8, 9 and 11 at Svartsengi geothermal field (Bjarnason, 1996)

Figure 25a demonstrates that *total dissolved solids* have shown no significant variation besides some slight declines around 1984 and 1994 which can be explained by enthalpy changes (steam gain). Quartz temperature remained constant, aside from some declines around 1982-84 and an increase in 1985 (Figure 25b). The decline in 1982-84 is attributed to boiling effects while the increase in 1985 might be due to increased contribution from deeper component fluids.

The *magnesium* concentration shows a generally declining trend attributed to the loss of CO_2 from the geothermal field (Figure 26a). When fluid boils from a hot temperature reservoir, it loses gases (CO_2 and H_2S) and consequently the pH rises. Thus Mg^{2+} should decrease as the pH rises due to degassing. Mg^{2+} is influenced by reservoir temperature, pH, and CO_2 concentration. The hydroxyl concentration rises with increasing pH and correlates positively with fluoride concentration (Figure 26b). The fluoride seems to be influenced by the hydroxyl ion concentration, probably through ion exchange reactions with some alteration minerals.

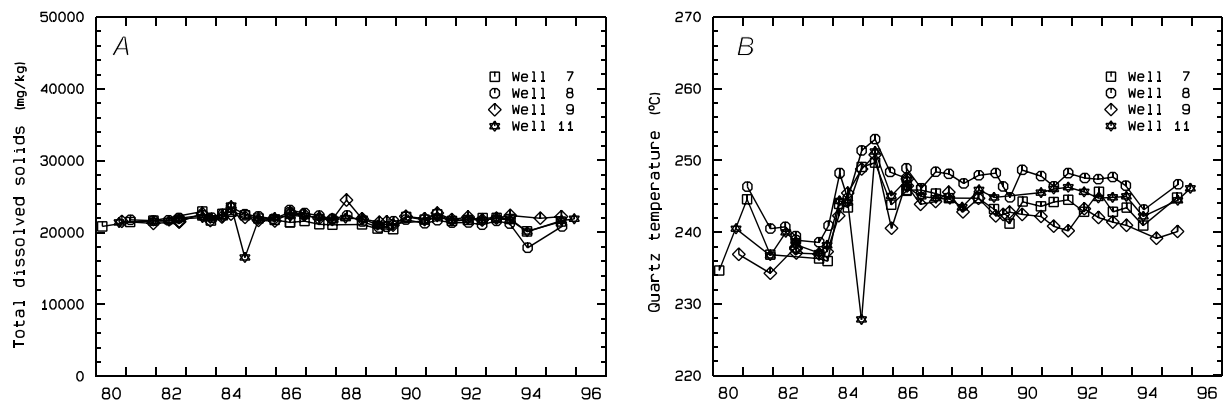


FIGURE 25: Temporal changes of A) TDS and B) Quartz temperature in geothermal fluids of wells 7, 8, 9 and 11 at Svartsengi geothermal field (Bjarnason, 1996)

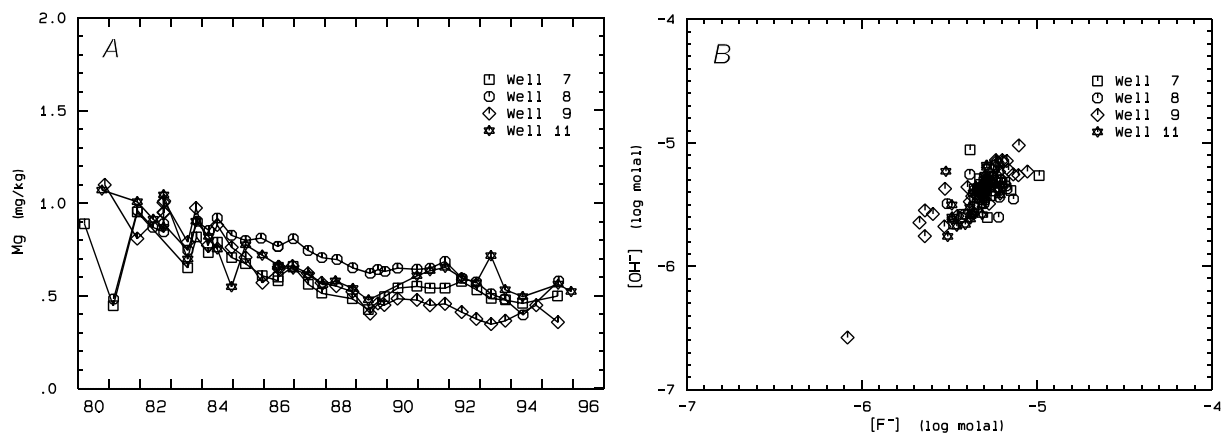


FIGURE 26: Temporal changes of A) magnesium (mg/kg) and B) hydroxyl versus fluorine plot in wells 7, 8, 9 and 11 at Svartsengi geothermal field (Bjarnason, 1996)

3.6 Conclusions

- Isotopic analysis indicates that the geothermal water is enriched in $\delta^{18}\text{O}$ by about 0.5‰ and depleted in δD by about 5‰ counter to what is expected from chemical analysis. This is attributed to water-rock interaction over time and it is suggested that at previous stage the circulating fluid was more dilute than today possibly during past glaciations. At that time the local precipitation on Reykjanes was lighter than at present due to colder climate and it is therefore possible that the light nature of the δD values at Svartsengi can be explained by “ice-age water” still circulating in the system. This would not be seen in the corresponding d^{18}O values due to the observed oxygen shift. The depletion in δD could also be attributed to isotopic exchange with hydrous minerals formed when the fluid was more dilute than today.
- Evidence of injection of freshwater is most obvious in well SG-6 where the lighter freshwater influenced the isotopic composition of the geothermal water.
- Geospatial isotopic data indicate $\delta^{18}\text{O}$ enrichment in a southwesterly direction. However, this trend changed to a northeastern direction between 1993-1994 as inferred by $\delta^{18}\text{O}$ enrichment in that direction. The former trend is attributed to injection of lighter freshwater in well SG-12 whilst the latter is probably due to progressive boiling in formation close to well SG-12 that might have created isotopically heavy residual water.

- Information on the temporal changes of the isotopic composition of geothermal water in Svartsengi geothermal field indicates a slight depletion in 1984. The above isotopic change is due to boiling phenomena that might have caused a steam gain in the discharge.
- The isotopic changes that are accompanied with small changes in chloride concentration can be explained by enthalpy changes (gain or loss of steam) or be due to slight variations in the underground chloride water.

ACKNOWLEDGEMENTS

I have to thank the International Atomic Energy Agency, Vienna for awarding me a fellowship to study the peaceful applications of atomic energy. It is my wish to acknowledge the Government of Uganda, which nominated me to enhance my professional capability and technical competence in geothermal exploration and development. My sincere thanks go to the Staff at Orkustofnun, UNU, which have trained me in all aspects of geothermal energy utilisation and development, in particular Director Dr. Ingvar. B. Fridleifsson and Mr. Lúdvík. S. Georgsson. Lúdvík, I owe you full credit; you undoubtedly enhanced my computer skills. I owe special thanks to Dr. Árný E. Sveinbjörnsdóttir who assisted me in planning and designing my project, supervised me, shared with me her experience and expertise in isotopic techniques and made it possible for me to finish my project in time. To Mr. H. Ármannsson, I extend my thanks for contributing information and reviewing this project. I acknowledge all the consulted sources of information, particularly Mr. J.Ö. Bjarnason for permission to use Svartsengi monitoring data. Finally, special thanks to my wife Robinah Nakamya, for the encouragement and endurance during the six months I was away from home.

REFERENCES

- Arad, A., and Marton, W.H., 1969: Mineral springs and saline lakes of western rift valley, Uganda. *Geochim. Cosmochim. Acta*, 33, 1169-1181.
- Ármannsson, H., 1994: *Geothermal studies on three geothermal areas in West and Southwest Uganda*. UNDESD, UNDP project UGA/92/002, report, 85 pp.
- Arnórsson, S., 1978: Major element geochemistry of the geothermal seawater at Reykjanes and Svartsengi. *Mineral Mag.*, 42, 209-220.
- Arnórsson, S., Gunnlaugsson, E., and Svavarsson, H., 1983: The chemistry of geothermal waters in Iceland III. Chemical geothermometry in geothermal investigations. *Geochim. Cosmochim. Acta*, 47, 567-577.
- Arnórsson, S., Sveinbjörnsdóttir, Á.E., and Andrésdóttir, A., 1993: *Processes influencing δD , $\delta^{18}O$, Cl and B distribution in cold and thermal waters in the NW-Peninsula and in the Southern Lowlands, Iceland*. International Atomic Energy Agency, report TEC-DOC-788, 45-61.
- Bjarnason, J.Ö., 1988: *Svartsengi chemical monitoring, 1980-1987*. Orkustofnun, Reykjavík, report OS-88001/JHD-01 (In Icelandic, with English summary), 98 pp.
- Bjarnason, J.Ö., 1994: *The speciation program WATCH, version 2.1*. Orkustofnun, Reykjavík, 7 pp.
- Bjarnason, J.Ö., 1995: *Chemical composition of freshwater, saltwater, and seawater in the Reykjanes area, SW Iceland*. Orkustofnun, Reykjavík, report JÖB-95/O4 (in Icelandic), 125 pp.

Bjarnason, J.Ö., 1996: *Svartsengi chemical monitoring, 1988-1995*. Orkustofnun, Reykjavík, report OS-96082/JHD-10 (in Icelandic, with English summary), 57 pp.

Björnsson, G., and Albertsson A., 1985: The power plant at Svartsengi. Development and experience. *Proceedings of the 1985 International Symposium on Geothermal Energy, Geothermal Resources Council, Davis*, 427-442.

Björnsson, G., and Steingrímsson, B., 1991: *Temperature and pressure in the Svartsengi geothermal reservoir*. Orkustofnun, Reykjavík, report OS-91016/JHD-04 (in Icelandic with English summary), 69 pp.

Björnsson G., and Steingrímsson., B., 1992: Fifteen years of pressure and temperature monitoring in the Svartsengi geothermal field, Iceland. *Geothermal Resource Council, Transactions*, 16, 627-634.

Clarke, M.C.G., Woodhall, D.G., Allen, D., and Darling, W.G., 1991: *Geological, volcanological and hydrogeological controls on the occurrence of geothermal activity in the area surrounding Lake Naivasha, Kenya*. Ministry of Energy, Nairobi, Kenya, report, 138 pp. + 3 maps.

Craig, H., 1961: Isotopic variations in meteoric water. *Science*, 133, 1702-1703.

EASD, 1996: *State of environment reporting in Uganda*. Chapter one, EASD. <http://easd.org.za/soe/Uganda/soechapt1.htm> .

Epstein, S., and Mayeda, T.K., 1953: Variation of $\delta^{18}\text{O}$ content of waters from natural sources. *Geochim. Cosmochim. Acta*, 4, 213-224.

Eysteinnsson, H., Árnason, K., Flóvenz, Ó.G., 1993: Resistivity methods in geothermal prospecting in Iceland. *Surveys in Geophysics*, 15, 263-275.

Fournier, R.O., and Potter, R.W. II, 1982: A revised and expanded silica (quartz) geothermometer. *Geoth. Res. Council Bull.*, 11-10, 3-12.

Franzson, H., 1983: The Svartsengi high-temperature field, Iceland - subsurface geology and alteration. *Geoth. Res. Council, Transactions*, 7, 141-145.

Friedman, I., 1953: Deuterium content of natural water and other substances. *Geochim. Cosmochim. Acta*, 4, 89-103.

Georgsson, L.S., 1981: A resistivity survey on the plate boundaries in the western Reykjanes peninsula, Iceland. *Geothermal Resources Council, Trans.* 5, 75-78.

Gudmundsson, J.S., 1983a: Geothermal electric power in Iceland: Development in perspective. *Energy* 8, 491-513.

Gudmundsson, J.S., 1983b: Silical deposition from geothermal brine at Svartsengi, Iceland. *Proc. Symp. Solving Corrosion-Scaling Problems in Geothermal Systems. San Francisco, California, January*, 72-87.

Gudmundsson, J.S., 1983c: Injection testing in 1982 at the Svartsengi high temperature field in Iceland. *Geothermal Resources Council, Trans.* 7, 423-428.

Gudmundsson, J.S., Hauksson, T., Thórhallsson, S., Albertsson, A., and Thórólfsson, G., 1984: Injection and tracer testing in Svartsengi geothermal field, Iceland. *Proceedings of the 6th New Zealand Geothermal Workshop, Geothermal Institute, Auckland*, 175-180.

Harris, N., Brown, J.M., and Pallister, J.W., 1956: *Oil in Uganda*. Geological Survey of Uganda, Memoir No. IX, 33 pp.

Henley, R.W., Truesdell, A., and Barton, P.B. Jr. H., 1984: *Fluid-mineral equilibrium in hydrothermal systems*. Society of Economic Geologists, Reviews in Economic Geology, 1, 267 pp.

Ingimarsson, J., Eliasson, J., and Kjaran, S.P., 1978: *Evaluation of groundwater level and maximum yield of wells in a fresh water lens in Svartsengi SW-Iceland*. Orkustofnun, Reykjavik, Report OS-SFS-7802, 10 pp.

Kendal, C., and Caldwell, E.A., 1998: *Fundamentals of isotope geochemistry*. Chapter 2, USGS, <http://wwwrcamnl.wr.usgs.gov/isoig/isopubs/itchch2.html>.

Kjaran, S.P., Eliasson, J., and Halldórsson, G.K., 1980: *Svartsengi, reservoir engineering studies of the exploitation of geothermal reservoir*. Orkustofnun, Reykjavik, Report OS-80021/ROD-10/JHD-17 (in Icelandic with English summary), 98 pp.

Kjaran, S.P., Halldórsson, G.K., Thórhallsson, S., and Eliasson, J., 1979: Reservoir engineering aspects of Svartsengi geothermal area. *Geothermal Resources Council, Trans.*, 3, 337-339.

Kristmannsdóttir H., and Mastubaya, O., 1995: Stable isotope interaction in geothermal systems on the Reykjanes peninsula, SW Iceland. *Proceedings of the 8th International Symposium on Water-Rock interaction, Vladivostok, Russia, 1995*, 199-202.

Logatchev, N.A., Belousov, V.V., and Milanovsky, E.E., 1972: East African Rift development. In: Girdler, R.W. (editor), East African Rifts. *Tectonophysics*, 15, 71-81.

Muehlenbachs, K. and Clayton, R.N., 1976: Oxygen isotope composition of the oceanic crust and its bearing on seawater. *J. Geophys. Res.*, 81-23, 4365-4369.

Pálmason, G., Stefánsson, V., Thórhallsson, S., and Thorsteinsson, Th., 1983: Geothermal field development in Iceland. *Proceedings of the 9th Workshop on Geothermal Reservoir Engineering*. Stanford University, California, 37-51.

Petroconsultants., 1971: *Geology and petroleum potential of Lake Edward-George and Lake Mobutu (Albert) rift area, Uganda*. Petroconsultant report.

Pullinger, C.P., 1991: *Geological and geothermal mapping at Nupafjall and Svartsengi in the Reykjanes Peninsula, SW-Iceland*. UNU G.T.P., Iceland, report 11, 45 pp.

Stefánsson, V., 1989: *Government of Uganda, mission report*. United Nations, New York, 29 pp.

Sveinbjörnsdóttir, Á.E., Coleman, M.L., and Yardley, B.W.D., 1986: Origin and history of hydrothermal fluids of the Reykjanes and Krafla geothermal fields, Iceland. A stable isotope study. *Contrib. Mineral. Petrol.* 94, 99-109.

Sveinbjörnsdóttir, Á.E., Johnsen, S., and Arnórsson, S., 1995: The use of stable isotopes of oxygen and hydrogen in geothermal studies in Iceland. *Proceedings of the World Geothermal Congress, 1995, Florence, Italy*, 2, 1043-1048.

Thórhallsson, S., 1979: Combined generation of heat and electricity from geothermal brine at Svartsengi in SW-Iceland. *Geothermal Resources Council, Trans.* 3, 733-736.

APPENDIX

TABLE 1: Chemical and isotopic data for geothermal areas in Uganda
(concentrations in mg/kg)

Location	Sample no.	T (°C)	pH/C	CO ₂	H ₂ S	Si ₂ O	Na	K	Ca	Mg	SO ₄	Cl	F	Fe	Al	B	Sr	Li	Br	Mn	TDS	δ ¹⁸ O (‰)	δD (‰)
Katwe-Kikorongo geothermal area																							
CS-13	1	28.6	7.61/26	156	0	29.3	44.7	35.1	10.1	5.92	7	3.9	0.75	0.004	0.007	0	0.26	0.003	0.04	0	132	-3.5	-9
CS-06	2	28.5	9.64/26	11316	5.3	88.6	25600	3500	0.1	0.95	9940	19000	8.52	0.13	0.03	1.9	0.17	0.067	149	0	72000	1.9	-6
CS-01	3	27.5	9.42/27	5523	0	32.2	8950	722	0.13	0.49	6450	3340	19.6	0.03	0.019	0.27	0.09	0.025	21.6	0.001	24690	1.12	9.1
LW-01	4	23.3	8.55/28	223	0	18.2	83.7	41.5	16.8	27.3	18	20.2	0.69	0.05	0.065	0	0.42	0.013	0.1	0.002	254	2.5	22.1
BH5455	5	26.6	6.95/27	1000	0	53.7	952	89.7	296	232	1800	723	0.68	0.04	0.02	0	4.35	0.023	5.4	0.002	4870	-1.8	-8
HS-05	6	66.6	8.41/26	3105	0	91	9310	644	0.6	0.85	13400	2430	42	0.02	0.01	0.82	0.59	0.063	14.2	0.001	27770	-0.7	0.5
HS-02	7	56.6	8.03/26	2544	0	105	6510	523	1.45	6.27	8970	1770	26.7	0.01	0.016	0.59	1.27	0.031	10.8	0.001	19410	-0.6	3.2
LW-02	8	26.2	8.28/27	108	0	21.5	38.5	7.8	22.9	11.2	11	10.3	0.36	0.02	0.014	0.06	0.31	0.005	0.07	0.007	180	0.98	12.6
HS-01	18	61.2	9.57/24	17785	40.7	351	84200	4740	0.9	0.74	108900	20900	402	0.02	0.073	7.6	1.8	0.21	120	0.012	244100	10	16.5
94-06	94-06	61.1	9.33	10350	19.4	210	33600	1840	4.1	2	44000	8370	162	0.025	0.48	2.77	3.6	0.16	44.8	0.003	99515	2.2	0
HS-01	27	70.1	9.72/27	5248	7.1	289.8	66600	3500	4	1.38	85300	16900	310	0.03	0.8	5.2	1.7	0.07	89.8	0.005	196000	7.4	25.3
LW-03	28	36	9.57/27	19470	0.3	389	87300	4780	4.3	1.47	110300	22200	398	0.04	1.28	6.9	1.6	0.08	122	0.016	256000	10	24
LW-04	29	28	9.55/30	9008	4.8	237.6	124500	22500	5.3	32.5	71300	86600	37.3	0.26	1.29	17.5	0.4	0.11	806	0.22	372000	9.6	24.5
LW-05	30	26.2	9.66/27	7368	0	149																	
Buranga geothermal area																							
HS-02	9	93.4	7.87/20	2445	0	76.9	5320	195	2.45	2.13	3720	3580	27.9	0.04	0.021	4.3	2.41	1.34	16.8	0.001	14600	-3.6	-17.1
HS-05	10	93.6	7.73/20	2411	0	76.4	5160	190	2.56	2.27	3570	3490	27.2	0.05	0.014	4.2	2.46	1.3	16.4	0.001	14030	-3.49	-12.8
HS-13	11	80.3	7.61/21	2889	0	88.6	6160	230	2.1	2.63	4330	4160	31.3	0.02	0.019	4.96	2	1.51	20	0.002	17050	-3.54	-12.4
HS-20	12	89	7.50/22	2798	0.3	81	5950	219	2.69	2.19	4160	4030	30.8	0.02	0.019	4.7	2.54	1.47	19.6	0.001	16400	-3.69	-12.7
HS-19	13	85.8	7.81/21	2878	0	85.7	6300	234	2.04	1.98	4420	4240	31.5	0.01	0.017	4.8	2.15	1.54	20.4	0	17050	-3.46	-12.9
HS-17	14	98.2	8.57/21	2635	0	85.1	6270	235	0.39	0.28	4400	4210	31.3	0.39	0.54	4.96	0.33	1.51	20.1	0.002	17080	-3.45	-13.4
SW	15	21.8	7.52/20	57	0	37.2	11.1	3.7	11.2	3.61	1.7	1.8	0.17	0.02	0.011	0	0.08	0.008	0	0	74	-2.24	-3.7
HS-09	16	95.8	8.15/20	2638	0	87.7	5940	222	0.95	1.74	4180	4010	29.9	0.01	0.025	4.71	0.86	1.48	19.3	0.001	16250	-3.21	-12.2
CS-01	17	23.8	7.54/20	197	0	36.3	21.2	8.1	54.7	14.3	27.6	2.1	0.36	0.00	0.005	0	0.31	0.034	0	0	208	-2.57	-4.6
Kibiro geothermal area																							
HS-02	19	86.5	7.06/24	146	10.4	129	1530	169	62	8.14	46.7	2500	5.12	0	0.037	2.26	2.1	1.5	16.7	0.004	4576	-2.01	11.3
HS-05	20	81.1	7.14/25	155	13	125	1490	164	62.9	7.96	26.4	2450	5.02	0.02	0.041	2.23	2.08	1.48	16.4	0.004	4436	-2.08	-11.8
HS-14	21	71.8	7.14/25	155	17.3	122	1480	165	65.7	9.21	15.4	2440	4.74	0	0.044	2.21	1.9	1.46	16.2	0.007	4384	-1.98	-10.6
HS-17	22	39.5	8.05/35	115	0	135	1570	182	75.9	8.71	49.9	2580	5.37	0.03	0.029	2.47	2.05	1.53	17.3	0.006	4548	-1.01	-3.9
LW-01	23	30	8.93/24	236	Nd	0.5	72.3	49.4	9.75	27.3	19.3	24.2	0.83	0.07	0.015	0	0.34	0.012	0.13	0	338	5.47	39.8
BH3803	24	29.8	6.89/22	367	Nd	90.5	87.5	7.7	75.8	39.5	139	31.2	0.37	1.5	0.01	0	0.36	0.016	0.26	0.001	662	-3.58	-15.2
BH1713	25	23.6	6.26/22	130	Nd	70.8	12.4	2.6	14.8	8.03	5.3	5.2	0.12	0.74	0.007	0	0.08	0.003	0.04	0.001	124	-1.57	-4.1
BH1646	26	24.9	6.72/22	232	Nd	76.1	50.6	7.5	138	39.5	227	123	0.12	0.72	0.014	0	0.44	0.015	0.64	0.034	680	-2.08	-5.2

Nd = Not determined, 0 = not detected, HS = Hot spring, LW = Lake water, CS = Cold spring, SW = Stream water

TABLE 2: Isotopic data for Kibiro geothermal area Uganda

SA-Code	$\delta^{18}\text{O}$ (‰)	δD (‰)	Longitude	Latitude	Altitude (m)	Cond (ms/cm)	Temp (°C)	pH	Alkali (mg/l)
001	-2.05	11.10	0311534E	014045N	675	7210	85	7.26	133
002	-1.79	-2.40	0311765E	013745N	1101	276	22	7.13	115
003	-1.65	-0.95	0311713E	013619N	1132	122	22	6.27	56
004	-1.58	-0.90	0311831E	013770N	1131	183	22	8.10	96
005	-1.46	-0.35	0311839E	013834N	1131	154	22	7.31	74
006	-1.57	-0.50	0311549E	013424N	1048	143	22	6.62	74
007	-0.47	8.15	0311834E	013584N	1058	26	23	7.37	30
008	-0.84	5.10	0311869E	013547N	1038	41	19	7.33	38
009	-2.48	-8.95	0311450E	013540N	989	714	23	7.60	280
010	-0.97	4.75	0310687E	013180N	992	70	19	7.50	28

Sample 001 = Hot spring sample; Samples 008 and 010 = River samples;
 Samples 002, 003, 004,005,006,009 = Bore hole samples; Sample 007 = Shallow well sample

TABLE 3: Chemical and isotopic monitoring data for Svartsengi geothermal field (concentrations in mg/kg) (Report OS-96082/JHD-10 Orkustofnun)

Well no.	Month	Year	$\delta^{18}\text{O}$ (‰)	δD (‰)	Cl	B	SiO ₂	H ₂ S	Lg/kgbv	Na	Ca	H ₂	CO ₂	pH/°C
6	June	1989	-2.27	-27.9	11860	7.3	466	0.07	0.8	6115	901	0.48	1549	6.63/25
6	Dec	1989	-2.01	-38.4	12210	7.55	462	0.45	0.81	6380	973	0.91	1776	6.68/23.3
7	May	1989	-1.55	-24.6	13125	7.96	484	0.55	0.79	6660	1047	0.15	1652	6.53/24.3
7	Nov	1989	-1.51	-	13060	8.12	469	0.14	0.98	6800	1036	0.24	1445	6.44/23.4
7	May	1991	-1.23	-	13680	8	488	0.74	1.45	6735	1080	0.25	1543	6.28/24
7	May	1992	-1.45	-23.6	13552	8.18	479.3	1.42	1.35	6970	1120	0.35	1937	6.28/25.7
7	Nov	1992	-1.5	-21.8	13440	8.18	496.8	0.65	1.33	6960	1160	0.45	1820	6.23/22.5
7	Oct	1993	-1.19	-30	13450	7.9	482	0.46	1.71	6970	1090	0.36	1530	6.24/25.3
7	May	1994	-1.3	-19.9	12500	7.54	467	0.27	1.42	6420	940	0.31	1780	6.19/23.7
8	June	1989	-1.59	-24.1	13100	7.89	515	0.74	1.14	6750	989	0.08	1356	6.24/25
8	Sept	1989	-1.54	-26.3	13175	8.07	502	0.74	1.02	6990	1001	0.1	1655	6.38/22.5
8	Dec	1989	-1.55	-	13040	7.91	493	0.9	1.33	6840	1024	0.07	1610	6.36/23.2
8	May	1991	-1.37	-	13500	7.96	504.2	0.69	0.93	6765	1042	0.12	1682	6.39/23.7
8	Nov	1992	-1.54	-22.6	13380	8.16	511.8	0.66	1.15	6910	1140	0.09	1857	6.53/21.9
8	Oct	1993	-1.33	-23.4	12720	7.64	507.5	0.32	1.04	6650	996	0.6	1878	6.4/22.4
8	May	1994	-1.32	-26	11500	6.5	490	0	0.86	5940	810	0	1600	6.52/23.9
9	June	1989	-1.44	-22.8	13675	7.93	477	0.79	0.68	6970	1062	0.1	1369	6.28/25
9	Sep	1989	-1.44	-21.1	13590	8	477	0.82	0.59	7200	1110	0.21	1455	6.47/22.5
9	Nov	1989	-1.42	-24	13530	8.04	479	0.49	0.69	7240	1126	0.21	1674	6.52/23.4
9	May	1991	-1.27	-	13945	7.9	468.3	0.39	0.54	6889	1125	0.22	1672	6.43/24.5
9	May	1992	-1.45	-20.8	13818	8.1	483.4	0.64	0.49	7110	1190	0.3	1660	6.61/25.1
9	Nov	1992	-1.5	-22.6	13690	7.97	476.4	0.57	0.32	7050	1230	0.5	1693	6.58/22.3
9	Oct	1993	-1.39	-24.9	13800	7.79	470	0.94	0.67	7110	1170	0.84	1456	6.44/24.8
9	Oct	1994	-1.43	-25.8	14000	7.75	458	0.51	0.3	7090	1200	0.38	1390	6.76/23.4
10	May	1989	-3.9	-22.4	1.76	0.16	16.9	33.4	5.1	2.18	2.51	0	1691	4.65/23.4
10	Nov	1989	-3.63	-22.5	0.57	0.17	4.22	35.4	14.1	0.38	0.88	0.21	1801	4.48/22.6
10	May	1991	3.29	-	0.17	0.13	1.93	60.5	9.98	0.26	0.87	0.3	1741	4.28/23.4
10	May	1992	-3.12	-22.4	0.13	0.19	0.69	47.6	54.5	0.46	1.02	0.32	1753	4.43/24
10	Nov	1992	-3.89	-23.6	2.38	0.34	2	59	-	0.55	0.85	0.37	2090	4.13/22.6
10	Nov	1993	-3.9	-30.4	0.38	0.1	0.7	93	-	0.24	0.22	0.38	1767	4.25/25
10	May	1994	-3.05	-21.6	0.27	0.37	1.15	41	14.8	0.3	0.18	0.36	1350	4.3/25.3
11	May	1989	-1.4	-27.2	13420	8.24	493	0.94	0.82	6830	1055	0.07	1783	6.24/24.2
11	May	1991	-1.34	-	13665	8.1	497.2	1.37	2.39	6827	1065	0.11	1725	5.98/24
11	May	1992	-1.44	-19.1	13547	8.35	495	1.33	1.79	7000	1120	0.41	1894	6.1/26.2
11	Nov	1992	-1.47	-22.2	13380	8.05	490.3	0.94	2.1	6860	1160	0.4	1633	6.13/22.3
11	Nov	1993	-1.37	-29.4	13170	7.86	492	0.91	2.33	6920	1060	0.22	1660	5.94/23.9
11	May	1994	-1.48	-24.5	12800	7.59	475	0.89	1.85	6500	960	0.56	1650	6.07/24.4
12	May	1989	-1.99	-26.3	12250	7.56	455	0	1	6400	889	0.27	1606	6.56/23.7
12	Nov	1989	-1.92	-27.2	12170	7.69	446	0.12	0.94	6440	879	0.49	1619	6.87/23.5
12	May	1991	-1.45	-	13260	7.92	453.3	0.48	0.9	6705	1034	0.42	1859	6.62/23.3
12	May	1992	-1.5	-21.4	13515	8.47	459	0.63	0.97	7030	1120	0.17	1737	6.62/26
12	Nov	1992	-1.45	-24.4	13600	8.38	468.2	0.41	1.07	7030	1160	0.3	1662	6.76/22.4
12	Oct	1993	-1.48	-27.4	13720	8.28	457.7	0.46	0.92	7130	1120	0.22	1644	6.67/23.4
12	May	1994	-0.92	-23.8	13800	8.25	448	0.33	0.78	7070	1090	0.16	1780	6.78/23.8

Discharge enthalpy of wells 5, 7, 8, 9, 11 = 1028 kJ/kg; discharge enthalpy of well 6 in 1989 = 986 kJ/kg;
 discharge enthalpy for well 12 = 995kJ/kg.